



VICTORIA UNIVERSITY
MELBOURNE AUSTRALIA

*Statistical Downscaling of General Circulation Model
Outputs to Precipitation - part 2: bias-correction and
future projections*

This is the Accepted version of the following publication

Dhanapala Arachchige, Sachindra, Huang, Fuchun, Barton, Andrew and Perera, B. J. C (2014) Statistical Downscaling of General Circulation Model Outputs to Precipitation - part 2: bias-correction and future projections. International Journal of Climatology. ISSN 1097-0088

The publisher's official version can be found at
<http://onlinelibrary.wiley.com/doi/10.1002/joc.3915/abstract>
Note that access to this version may require subscription.

Downloaded from VU Research Repository <https://vuir.vu.edu.au/24326/>

Statistical downscaling of general circulation model outputs to precipitation – part 2: bias-correction and future projections

D. A. Sachindra,^{a*} F. Huang,^a A. Barton^{a,b} and B. J. C. Perera^a

^a College of Engineering and Science, Footscray Park Campus, Victoria University, Melbourne, Australia

^b School of Science, Information Technology and Engineering, University of Ballarat, Victoria, Australia

ABSTRACT: This article is the second of a series of two articles. In the first article, two models were developed with National Centers for Environmental Prediction/National Center for Atmospheric Research (NCEP/NCAR) reanalysis and HadCM3 outputs, for statistically downscaling these outputs to monthly precipitation at a site in north-western Victoria, Australia. In that study, it was seen that the downscaling model developed with NCEP/NCAR reanalysis outputs performs much better than the model developed with HadCM3 outputs. Furthermore, it was found that there is large bias in HadCM3 outputs which needs to be corrected. In this article, the downscaling model developed with NCEP/NCAR reanalysis outputs was used to downscale HadCM3 20th century climate experiment outputs to monthly precipitation over the period 1950–1999. In all four seasons, the precipitation downscaled with HadCM3 20th century outputs, displayed a large scatter and the majority of precipitation was overestimated. The precipitation downscaled with HadCM3 outputs was bias-corrected against the observed precipitation pertaining to the period 1950–1999, using three techniques: (1) equidistant quantile mapping (EDQM), (2) monthly bias-correction (MBC) and (3) nested bias-correction (NBC). Although all these bias-correction techniques were able to adequately correct the statistics of downscaled precipitation, the magnitude of the scatter of precipitation remained almost the same. Considering the performances and its ability to correct the cumulative distribution of precipitation, EDQM was selected for the bias-correction of future precipitation projections. HadCM3 outputs for the A2 and B1 greenhouse gas scenarios were introduced to the downscaling model and the downscaled precipitation for the period 2000–2099 was bias-corrected with the EDQM technique. Both A2 and B1 scenarios indicated a rise in the average of future precipitation in winter and a drop in it in summer and spring. These scenarios showed an increase in the maximum monthly precipitation in all seasons and an increase in percentage of months with zero precipitation in summer, autumn and spring.

KEY WORDS statistical downscaling; precipitation; general circulation model; bias

Received 10 December 2012; Revised 19 July 2013; Accepted 5 December 2013

1. Introduction

Over the 800 000-year period prior to the industrial revolution (1750–1850), the concentration of the atmospheric carbon dioxide [dominant greenhouse gas (GHG)] fluctuated approximately between 180 and 280 parts per million (ppm) (Tripathi *et al.*, 2009). Since the industrial revolution, owing to the consumption of fossil fuels, the concentration of the global mean atmospheric carbon dioxide level rose from 280 to 397 ppm by April 2013 (Earth System Research Laboratory, 2013). The rising concentrations of GHGs (mainly carbon dioxide) have increased the greenhouse effect leading to human-induced climate change, which is no longer a hypothetical phenomenon

(Hughes, 2003). As stated by Dessai *et al.* (2005), the global climate is expected to change throughout the 21st century. Climate change has shed its impacts, on humans as well as flora and fauna in many different ways. Impacts of climate change on health of humans (Thomas *et al.*, 2012), agricultural food production (Ziska *et al.*, 2012), floods (Prudhomme *et al.*, 2013) and water resources (Arnell and Gosling, 2013) are only some of the multitude of themes discussed in the literature.

General circulation models (GCMs) are the prime tools used in the projection of climate into the future (Fu *et al.*, 2012). GCMs are based on the theories of atmospheric physics. They are forced with plausible realizations on future GHG concentrations, in order to produce projections on global climate into future. The coarse resolution of GCM outputs hinders their direct use in catchment scale studies (Iizumi *et al.*, 2011). Downscaling techniques are used to link the coarse resolution GCM outputs with the catchment scale climatic variables. All downscaling techniques are based on the assumption that large-scale climate represented in GCM outputs is

*Correspondence to: D. A. Sachindra, College of Engineering and Science, Footscray Park Campus, Victoria University, P.O. Box 14428, Melbourne, Victoria 8001, Australia.
E-mail: sachindra.dhanapalaarachchige@live.vu.edu.au

[The copyright for this article was changed on 30 October 2014 after original online publication].

influential on the catchment scale hydroclimatology (Maraun *et al.*, 2010). There are two broad classes of downscaling techniques, namely; dynamic downscaling and statistical downscaling. In order to obtain local-scale climatic information, dynamic downscaling approaches employ regional climate models (RCMs) nested in GCMs (Murphy, 1998). Dynamic downscaling techniques are associated with high computational costs (Sun and Chen, 2012) due to the complex physics-based structure of the RCMs. However, owing to the use of physics-based equations to relate the predictors (GCM outputs which are used as input to downscaling models) with predictands (outputs of downscaling models – e.g. precipitation), dynamic downscaling techniques are capable in producing more reliable climatic information at local scale. This is because it is reasonable to assume that the same physics which was valid for the climate in the past is also valid for the climate in the future. On the other hand, statistical downscaling techniques are dependent on the empirical relationships developed between the GCM outputs and local-scale hydroclimatic variables. Statistical downscaling methods are computationally more efficient, due to the simplicity in their structure. In statistical downscaling techniques, it is assumed that the relationships derived between the predictors and predictands for the past observed climate are also applicable for the possible future climate (Iizumi *et al.*, 2011). However, the validity of this assumption cannot be tested at present as the future climate has not yet occurred (Chu *et al.*, 2010).

Statistical downscaling techniques are grouped under three classes; regression methods, weather typing (classification) and weather generators (Wilby *et al.*, 2004). In regression-based downscaling methods either linear or nonlinear relationships between the predictors and the predictand of interest are developed. By far, the regression-based methods are regarded as the most widely used statistical downscaling techniques (Nasseri *et al.*, 2013). Meenu *et al.* (2013) used the multi-linear regression (MLR) technique for downscaling GCM outputs to daily precipitation and then the downscaled precipitation was used in a hydrologic model to simulate streamflows. Samadi *et al.* (2013) used the MLR technique and artificial neural networks (ANN; nonlinear regression method) for downscaling GCM outputs to daily precipitation and temperature. They commented that the MLR-based downscaling technique was more capable than the ANN-based downscaling method in reproducing the observations of precipitation and temperature. Ghosh and Katkar (2012) employed MLR, ANN and support vector machine (SVM; nonlinear regression method) for downscaling GCM outputs to monthly precipitation. In that study, it was found that though the three regression-based downscaling models displayed similar overall performances in the calibration phase, the ANN-based model was able to better capture the relatively low and medium precipitation values and the SVM-based model was better at simulating relatively high values of precipitation.

In weather classification methods, patterns of large-scale weather characterized by a global or a regional

model are linked to a local-scale weather variable. Method of meteorological analogues is a widely used weather classification technique (Timbal *et al.*, 2009; Shao and Li, 2013). Also recursive partitioning is another classification type downscaling method (Schnur and Lettenmaier, 1998). Charles *et al.* (2013) used the method of meteorological analogues for downscaling GCM outputs to precipitation. It was found that this method was able to correct the bias in statistics of seasonal precipitation and also the number of wet days simulated by the GCM. In weather generation techniques, weather data for future are produced by scaling the parameters of the weather generator either up or down according to the changes in the GCM outputs pertaining to future. As an example the simplest weather generator for daily precipitation could have two parameters: (1) the probability of occurrence of a wet day and (2) the precipitation amount. In such case, the percentage changes in the parameters characterized by the GCM for the future climate with respect to those in the baseline period are determined. Then the values of the parameters pertaining to observed precipitation of the baseline period are scaled corresponding to the above determined changes. The new scaled parameters are used to generate time series of occurrence of wet days and precipitation amounts at the station of interest that reflects the large-scale changes in the precipitation simulated by the GCM. Applications of weather generation techniques are detailed in the studies of Chen *et al.* (2012) and Fatichi *et al.* (2011).

The classification of statistical downscaling techniques detailed by Maraun *et al.* (2010) separates the statistical downscaling techniques into three different categories: (1) perfect prognosis, (2) model output statistics (MOS) and (3) weather generators. Perfect prognosis methods involve establishing statistical relationships between the large-scale atmospheric variables and the catchment scale hydroclimatic variables, using regression techniques or weather classification approaches. In MOS methods, statistical relationships between the outputs of a RCM or a weather model and catchment scale observations of a predictand are used to improve the model outputs.

Although GCMs are regarded as the best tools available for projection of climate into the future, there are biases in GCM outputs. GCM bias is simply explained as the deviation of GCM outputs from the observations (Salvi *et al.*, 2011). However, in more elaborated terms, incorrect reproduction of extreme temperatures, prediction of excess number of wet days with low-intensity rainfalls, under or over-prediction of climatic variables, incorrect seasonal variations and so on are some of the forms of biases prevailing in GCM outputs (Teutschbein and Seibert, 2012). Chen *et al.* (2011) defined GCM bias as a time-independent component of the error in GCM outputs. According to Ojha *et al.* (2012), GCMs often incorrectly estimate the occurrences and intensities of precipitation. The limited understanding of the atmosphere and the simplified representation of the atmospheric processes in GCMs are regarded as the main causes of GCM bias (Li *et al.*, 2010). In general,

prognostic variables of a GCM contain relatively less bias than the diagnostic variables that are derived from the prognostic variables. Since prognostic variables do not always show good relationships with the predictands of interest, diagnostic variables are also used in developing the downscaling models despite their larger bias. The correction of bias is performed in two distinct ways: (1) the correction of bias in GCM outputs and (2) the correction of bias in the predictands (e.g. precipitation) which were downscaled from GCM outputs. However, neither of the above approaches is capable of correcting the inherent physics and thermodynamics of the GCM simulations, as bias-correction has no direct connection with the internal functions of the GCM. There are number of different bias-correction techniques in use, which are applicable to GCM outputs and also to the predictands downscaled from GCM outputs.

Ojha *et al.* (2012) reported that the bias seen in the GCM outputs should be corrected before their subsequent use. Johnson and Sharma (2012) used the nested bias-correction (NBC) for correcting the bias in monthly precipitation outputs of GCMs, over Australia. NBC corrects the bias in means, standard deviations and lag 1 autocorrelations of GCM outputs, simultaneously at both monthly and annual time scales. They commented that the NBC is successful when the bias in GCM outputs is not very large. Ojha *et al.* (2012) applied both NBC and monthly bias-correction (MBC) for removing the bias in precipitation outputs of number of GCMs, over India. Unlike the NBC described earlier, in the monthly bias-correction, only the means and standard deviations of the monthly GCM outputs are corrected with respect to those of the observations. In both nested and monthly bias-corrections, the statistics of the observed climatic data and the corresponding statistics of the past GCM outputs are used in the correction of the GCM outputs pertaining to future. These two methods assume that the biases in the model outputs for the past climate will remain same for the future climate (Johnson and Sharma, 2012).

Wood *et al.* (2004) employed the quantile mapping technique for bias-correcting the monthly precipitation and temperature outputs of a GCM. The quantile mapping (Panofsky and Brier, 1968) is a technique which can match all statistical moments of GCM outputs with those of observations, as in this technique cumulative distribution functions (CDFs) of GCM outputs for the past are mapped onto the CDF of the past observations. For the correction of bias in the GCM outputs pertaining to the future climate, first, corresponding to the values of the climatic variable for the future projections, the CDF values are obtained from the CDF which was derived from the past GCM simulations. Then pertaining to these CDF values, the bias-corrected values of the climatic variable for the future climate are extracted from the CDF of the observations of the past. Piani *et al.* (2010) used a gamma distribution-based quantile mapping technique for the bias-correction of daily precipitation downscaled by the RCM over Europe. It was concluded that this bias-correction is capable of correcting the average and the

other statistical moments of precipitation and also the statistical properties such as precipitation intensity. Lafon *et al.* (2013) applied four bias-correction techniques (linear scaling, nonlinear scaling, gamma distribution-based quantile mapping and empirical distribution-based quantile mapping) to reduce the bias in daily precipitation simulated by the RCM over the UK. They commented that all bias-correction techniques were able to correct the average and the standard deviation of daily precipitation with a good degree of accuracy. However, the accuracy of higher-order moments such as skewness and kurtosis of daily precipitation were sensitive to the bias-correction method and also to the period selected for the calibration of the bias-correction. Out of the four bias-correction techniques, the empirical distribution-based quantile mapping was identified as the best performing bias-correction. Gudmundsson *et al.* (2012) compared the performances of three variants of quantile mapping: distribution-derived, parametric and nonparametric (empirical distribution based quantile mapping) in correcting the bias in daily precipitation simulated by the RCM over Norway. They also concluded that nonparametric (empirical) quantile mapping is more effective in reducing the bias in precipitation. Themeßl *et al.* (2011) applied several bias-correction approaches to daily precipitation of the RCM over the Alps region in Europe. It was concluded that the empirical distribution-based quantile mapping technique displayed better performance than the other methods, particularly in correcting the extremes of precipitation.

Li *et al.* (2010) introduced a modified version of the quantile mapping technique called equidistant quantile mapping (EDQM). In equidistant quantile mapping, the difference between the CDF of the GCM output (to be corrected) and the CDF of the reference dataset (which can be field observations, reanalysis outputs, etc.), of the past climate, was subtracted from the CDF of the GCM output for future climate, for the bias-correction of future GCM outputs. In quantile mapping and equidistant quantile mapping, the CDFs of GCM outputs are corrected against the CDF of observations, therefore all statistical moments are explicitly corrected. On the other hand, NBC explicitly attempts to remove bias in the average, the standard deviation and the lag 1 autocorrelation of GCM outputs, and monthly bias-corrections reduces the bias in the average and the standard deviation only.

Ines and Hansen (2006) used the quantile mapping technique and the multiplicative shift method for bias-correction of daily mean precipitation output of a GCM. The multiplicative shift method involved the multiplication of daily precipitation output of the GCM by the ratio between the long-term observed and monthly precipitation output of the GCM. It was found that although this technique corrects the long-term observed monthly mean precipitation, it cannot correct any systematic error in the precipitation distribution. A regression-based bias-correction was employed by Kharin and Zwiers (2002) for the removal of bias from precipitation outputs of a

GCM. There a regression equation was built between the mean of the precipitation outputs of the GCM and observed precipitation, to correct the bias.

Above stated bias-correction techniques can be applied not only to GCM outputs, but also to the outputs of downscaling models, irrespective of whether the downscaling approach is dynamic or statistical. Ghosh and Mujumdar (2008) used the quantile mapping technique for the removal of bias in streamflows, which were statistically downscaled from GCM outputs. Teutschbein and Seibert (2012) used multiple bias-correction techniques (linear scaling, local intensity scaling, power transformation, variance scaling, quantile mapping and delta-change approach) on dynamically downscaled precipitation and temperature. The major advantage of applying the bias-correction techniques on the downscaled (either statistically or dynamically) hydroclimatic outputs is that, this process is computationally much cheaper than bias-correcting each GCM output individually, prior to downscaling. The advantage of applying a bias-correction to each GCM output separately (before introducing to the downscaling model) is that the bias in each variable is individually corrected. However, this procedure is useful only if the bias-correction was capable in adequately correcting the time series of each GCM output, rather than just their statistics.

The first article of this series of two articles which was entitled 'Statistical Downscaling of General Circulation Model Outputs to Precipitation. Part 1: Calibration and Validation' presented the calibration and validation of two statistical downscaling models, based on the MLR technique. In that study, the first model was developed with National Centers for Environmental Prediction/National Center for Atmospheric Research (NCEP/NCAR) reanalysis outputs and the second model was with Hadley Centre Coupled Model version 3 GCM (HadCM3) outputs. In both cases these outputs were used as the inputs to the downscaling models. According to the results of that study, it was seen that the model calibrated and validated with NCEP/NCAR reanalysis outputs was more capable in reproducing the observed precipitation, than its counterpart model which was built with HadCM3 20th century climate experiment outputs. Furthermore, a comparison of exceedance probability curves for the observed precipitation, precipitation reproduced by the downscaling models with NCEP/NCAR and HadCM3 outputs, and the raw precipitation output of HadCM3 model for 20th century climate experiment, over the period 1950–1999, revealed that there is large bias in the raw precipitation output of HadCM3 model. Therefore the need of a bias-correction was understood.

This article which is the second of the series of two articles, discusses the bias-correction and future precipitation projections of the statistical downscaling model developed in the first article, with NCEP/NCAR reanalysis outputs. This downscaling model was used in this study because of its better performances seen in the first article. The same MLR equations (with the same coefficients and constants) derived during the calibration

phase of this downscaling model were used in this study. Here onwards in this article, this model is referred to as the 'downscaling model'. Initially, the downscaling model was used to downscale the 20th century climate experiment outputs of HadCM3, to monthly precipitation. Then these downscaled precipitation data were bias-corrected against the observed precipitation (reference dataset for the bias-correction). For this purpose, three bias-correction techniques, namely (1) EDQM, (2) MBC and (3) NBC were employed. As a demonstration, the above procedure was applied to a precipitation station in the Grampians water supply system in north-western Victoria, Australia. The same station was also used in the first article. A performance comparison of the above three bias-corrections, derived from the above demonstration, is presented in this article. Considering the performances of each of these three bias-corrections, only the EDQM technique was used for the bias-correction of monthly precipitation projections produced into future by the downscaling model with HadCM3 outputs pertaining to the future climate. In downscaling GCM outputs to monthly precipitation, characteristics of precipitation such as occurrences of wet and dry days, extreme precipitation events, precipitation intensity are not captured. Though such characteristics are important in certain hydrological exercises, monthly precipitation is more useful in water resources management operations such as determining the optimum water allocation to crops, recreational facilities, domestic and industrial needs and to the environment particularly in the planning stage of a water resources project.

Section 2 of this article provides a brief description of the study area and the data used in the study. Section 3 describes the generic methodology, and its application with the results is detailed in Section 4. In Section 5, a summary of this work is provided along with the conclusions derived from this study.

2. Study area and data

The precipitation station located at the Halls Gap post office (Lat. -37.14° , Lon. 142.52° , elevation from the mean sea level about 236 m) in the Grampians water supply system of north-western Victoria, Australia was used as the case study station. The Grampians system is a multi-reservoir system owned by the Grampians Wimmera Mallee Water Cooperation (www.gwmwater.org.au).

Observed daily precipitation data from 1950 to 1999 were obtained from the SILO database (<http://www.longpaddock.qld.gov.au/silo/>) of Queensland Climate Change Centre of Excellence and these data were added to monthly precipitation totals. These monthly observations were used for the evaluation of the downscaling model when it was run with HadCM3 20th century climate experiment outputs and NCEP/NCAR reanalysis outputs. Also the observed precipitation was used as the reference dataset for the bias-correction. Monthly outputs

produced by HadCM3 GCM for the 20th century climate experiment were obtained from the Programme for Climate Model Diagnosis and Inter-comparison (PCMDI) (<https://esgceet.llnl.gov:8443/index.jsp>) for the period 1950–1999, and for the same period NCEP/NCAR reanalysis outputs were obtained from <http://www.esrl.noaa.gov/psd/>, for providing the inputs to the downscaling model in reproducing the observed precipitation.

The HadCM3 outputs corresponding to the COMMIT GHG emission scenario were extracted from the PCMDI website (<https://esgceet.llnl.gov:8443/index.jsp>) for the period 2000–2099, to validate the performances of the bias-correction. The COMMIT GHG emission scenario assumed that the GHG concentrations at year 2000 are constant throughout the period 2000–2099. Therefore, it was assumed that the statistics of future precipitation (2000–2099) downscaled from the outputs of HadCM3 pertaining to COMMIT scenario will closely reflect the statistics of the past precipitation (1950–1999) simulated by HadCM3. For the future projections of precipitation at the station selected, monthly outputs of the HadCM3 GCM under the A2 and B1 scenarios (IPCC, 2000), defined in the Special Report on Emission Scenarios (SRES) of the Intergovernmental Panel on Climate Change (IPCC) were obtained from the PCMDI website (<https://esgceet.llnl.gov:8443/index.jsp>) for the period 2000–2099. A2 and B1 GHG emission scenarios described a world with rapid economic growth and a world with greater focus on environmental protection, respectively.

3. Generic methodology

The reproduction of observed precipitation at the station of interest using the downscaling model with the 20th century climate experiment outputs of the GCM is explained, in subsection 3.1. Also this subsection details the procedure followed in downscaling the future precipitation using the downscaling model. Subsection 3.2 describes the bias-correction of the past and future downscaled precipitation, against the observed precipitation.

3.1. Reproduction of past precipitation and projection of precipitation into future with GCM outputs

For each calendar month, GCM outputs of the 20th century climate experiment were standardized with the corresponding means and standard deviations of reanalysis outputs (used for the model development) relevant to the calibration period of the downscaling model. In the calibration of the downscaling model, the reanalysis outputs were standardized with their means and standard deviations pertaining to the calibration period. Hence, these means and standard deviations became fixed parts of the model. These standardized GCM outputs of the 20th century climate experiment were introduced to the downscaling model, for reproducing the past observed precipitation. In the same way, the standardized reanalysis outputs were introduced to the downscaling

model for the reproduction of the past observed precipitation. The use of both GCM outputs of the 20th century climate experiment and reanalysis outputs enabled finding the capabilities of this model in reproducing past observations with these two sets of inputs obtained from two different sources. This was important as the downscaling model was developed with reanalysis outputs (refer to the first article of this series of articles) and it is used with GCM outputs in producing the projections into future.

The future GCM outputs for different GHG emission scenarios were standardized with the means and the standard deviations of reanalysis outputs (corresponding to calibration period of the downscaling model) for each calendar month and introduced to the downscaling model, for the projection of precipitation at the station of interest.

3.2. Bias-correction

The precipitation downscaled by the above model with GCM outputs was bias-corrected against the observed precipitation pertaining to the station of interest. The bias-correction was applied to the precipitation downscaled with GCM outputs as it was computationally efficient than bias-correcting each GCM output individually. Since the bias-correction techniques can be a source of uncertainty in statistical downscaling, Chen *et al.* (2011) investigated the use of several bias-correction techniques. Therefore, in this study the bias-correction was performed with three techniques: (1) EDQM, (2) MBC and (3) NBC. All these bias-correction techniques were applied separately on each calendar month and then for each technique the bias-corrected precipitation of each month was combined to produce the individual series. Bias-correction was performed for each calendar month in order to preserve the statistical attributes of precipitation in each calendar month. Considering the performances of these three bias-correction techniques, the best technique was identified. Thereafter the performances of the best bias-correction technique were validated. This was performed by comparing the statistics of the past observed precipitation with those of bias-corrected precipitation downscaled for a future GHG emission scenario (in this study the COMMIT scenario) which assumed that the GHG emission levels at the end of the 20th century remained constant throughout the 21st century. Owing to the above assumption it was assumed that this scenario which is pertaining to future could represent the statistics of the past climate simulated by the GCM closely. Following the validation, this bias-correction method was applied for the future precipitation projections produced by the downscaling model with GCM outputs.

3.2.1. Equidistant quantile mapping

EDQM (Li *et al.*, 2010) is a variant of the quantile mapping technique (Panofsky and Brier, 1968). In the EDQM technique, initially, the empirical CDFs were derived for the observed precipitation and precipitation downscaled with GCM outputs, for the past climate. Then the empirical CDF was developed for the precipitation

downscaled with GCM outputs, for the future climate under a GHG emission scenario. The periods which represented the past climate and the future climate were designated as period 1 and period 2, respectively.

The EDQM technique was applied in accordance with the following three steps (Salvi *et al.*, 2011). These three steps are graphically illustrated in Figure 1. In this figure, CDF1 and CDF2 correspond to the observed precipitation and precipitation reproduced by the downscaling model with GCM outputs respectively, for the past climate. CDF3 denotes the precipitation projected by the downscaling model with GCM outputs for a certain future GHG emission scenario. It should be noted that although this bias-correction technique corrects the CDF of the hydroclimatic variable, it does not explicitly correct the time series of the hydroclimatic variable.

3.2.1.1. Step 1: For a given precipitation value a_1 , the value c_1 was found from CDF2 (see Step 1 in Figure 1). From CDF1, the precipitation value a_2 that corresponded to c_1 was determined (see Step 1 in Figure 1). a_2 is the corrected precipitation value of a_1 . This corrective procedure was repeated for all precipitation values represented by CDF2. In other words, CDF2 was mapped onto CDF1. Once this mapping was performed, all the statistical properties of precipitation represented by CDF2 were automatically matched with those of CDF1. Hence, this step yielded the corrected CDF2 which exactly overlapped CDF1.

3.2.1.2. Step 2: Corresponding to a precipitation value b_1 , value c_2 was found from CDF3 (see Step 2 in Figure 1). Pertaining to that CDF value c_2 , the difference of precipitation (d) between CDF3 (future climate) and CDF2 (past climate) was computed (the sign of d was also considered), as shown in Step 2 in Figure 2.

3.2.1.3. Step 3: The difference d (considering its sign) calculated in Step 2 pertaining to CDF value c_2 was added to the corrected version of CDF2 (or CDF1) yielded in Step 1. This produced the bias-corrected precipitation value b_2 corresponding to its original value of b_1 . Steps 2 and 3 were repeated until all the future precipitation values represented in CDF3 were corrected. The negative precipitation values yielded in the corrected CDF3 were set to zero. In order to obtain the same result described in Steps 2 and 3, alternatively, the difference between CDF2 and CDF1 could be subtracted from CDF3, in order to bias-correct CDF3 (Li *et al.*, 2010).

3.2.2. Monthly bias-correction

MBC is a relatively simple bias-correction method used by Johnson and Sharma (2012). In that study, it was used to correct the mean and the standard deviation of the precipitation output of a GCM with those of the observed precipitation. In this study, it was employed to correct the mean and the standard deviation of the precipitation

downscaled with GCM outputs against those of observed precipitation.

Let monthly time series of precipitation downscaled with GCM outputs for a calendar month i be Y_i , for the past climate. As a first step, Y_i was standardized with its monthly mean ($\mu_{GCM,i}$) and standard deviation ($\sigma_{GCM,i}$) according to Equation (1). This yielded the standardized time series Y_i' for each calendar month as follows:

$$Y_i' = \frac{Y_i - \mu_{GCM,i}}{\sigma_{GCM,i}} \tag{1}$$

Then this standardized precipitation time series for each calendar month i (Y_i') was transformed back with Equation (2), using the monthly mean ($\mu_{Obs,i}$) and standard deviation ($\sigma_{Obs,i}$) of observed precipitation pertaining to the past climate. Equation (2) provided the monthly bias-corrected time series of precipitation downscaled with GCM outputs (Z_i). This bias-corrected time series of downscaled precipitation has the monthly mean and standard deviation of the observed precipitation.

$$Z_i = Y_i' \cdot \sigma_{Obs,i} + \mu_{Obs,i} \tag{2}$$

For the correction of bias in future precipitation, the precipitation downscaled with GCM outputs for future were standardized with their means and standard deviations corresponding to the past climate following Equation (1), and transformed back with those of past observed precipitation according to Equation (2). In MBC, it is assumed that the bias in the mean and the standard deviation of the precipitation downscaled with GCM outputs for past climate (with respect to past observations) remains the same in the future. This assumption is also valid for the NBC detailed in the next subsection. In MBC, though the mean and the standard deviation of the precipitation downscaled with GCM outputs were explicitly corrected, the CDF of the precipitation was not corrected. Therefore, the CDF of precipitation downscaled with GCM outputs for the past, was different from that of observed precipitation. This fact was also valid for the NBC, explained in the following section.

3.2.3. Nested bias-correction

NBC, proposed by Johnson and Sharma (2012), is a more complex bias-correction technique than the monthly bias-correction. While the MBC corrects the mean and the standard deviation in each calendar month, NBC corrects the mean, the standard deviation and the lag 1 autocorrelations, simultaneously at both monthly and annual time scales.

Like in MBC, in NBC, first the time series of precipitation downscaled with GCM outputs (for past climate) for each calendar month (Y_i) was standardized according to Equation (1). Then the lag 1 auto correlations ($\Omega_{GCM,i}$) in the above standardized precipitation time series were replaced with the corresponding lag 1 auto correlations

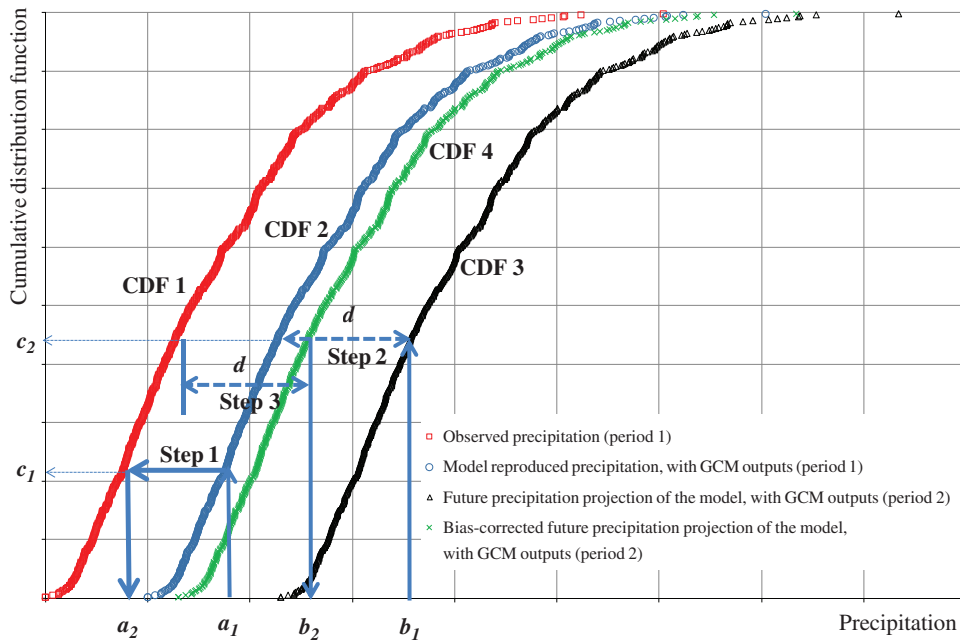


Figure 1. Equidistant quantile mapping.

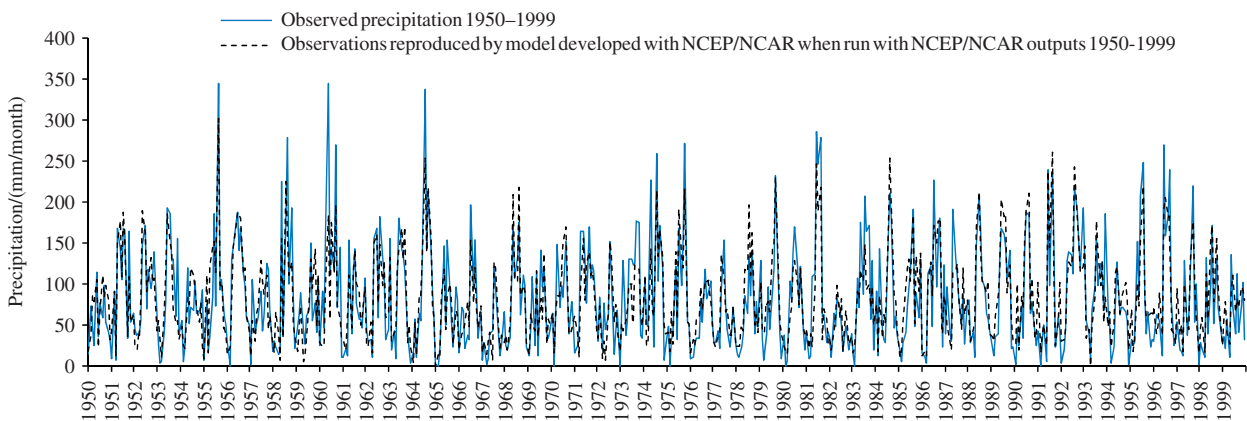


Figure 2. Time series plot for downscaling model run with NCEP/NCAR outputs as inputs (1950–1999).

in the observed precipitation ($\Omega_{Obs,i}$) to produce Y_i'' as shown in Equation (3). Lag 1 auto correlation for month i was calculated as the correlation between the monthly precipitation time series of month i and month $i - 1$.

$$Y_i'' = \Omega_{Obs,i} \cdot Y_{i-1}'' + \sqrt{1 - \Omega_{Obs,i}^2} \cdot \left(\frac{Y_i' - \Omega_{GCM,i} Y_{i-1}'}{\sqrt{1 - \Omega_{GCM,i}^2}} \right) \quad (3)$$

Then Y_i'' was transformed back with the mean ($\mu_{Obs,i}$) and the standard deviation ($\sigma_{Obs,i}$) of observed precipitation for each calendar month, as shown in Equation (4).

$$Y_i''' = Y_i'' \cdot \sigma_{Obs,i} + \mu_{Obs,i} \quad (4)$$

The bias-corrected monthly time series of downscaled precipitation yielded in Equation (4) has the monthly lag

1 auto correlations, the mean and the standard deviation of the observed precipitation.

Next, these rescaled monthly precipitation time series (Y_i''') in Equation (4) were summed to produce annual precipitation (Z_j) for each year j . This annual time series of precipitation was standardized with annual mean (μ_{GCM}) and standard deviation (σ_{GCM}) of the precipitation downscaled with GCM outputs, following Equation (5).

$$Z_j' = \frac{Z_j - \mu_{GCM}}{\sigma_{GCM}} \quad (5)$$

Thereafter, the annual lag 1 autocorrelations in Z_j' were replaced with those in the observed precipitation (Ω_{Obs}) to produce Z_j'' as shown in Equation (6). The annual lag 1 autocorrelations were computed as the correlation between precipitation in a certain year and

the following year.

$$Z_j'' = \Omega_{\text{Obs}} \cdot Z_{j-1}'' + \sqrt{1 - \Omega_{\text{Obs}}^2} \cdot \left(\frac{Z_j' - \Omega_{\text{GCM}} \cdot Z_{j-1}'}{\sqrt{1 - \Omega_{\text{GCM}}^2}} \right) \quad (6)$$

The annual time series modified in Equation (6) was rescaled with the annual mean (μ_{Obs}) and the annual standard deviation (σ_{Obs}) of observed precipitation time series, as given in Equation (7).

$$Z_j''' = Z_j'' \cdot \sigma_{\text{Obs}} + \mu_{\text{Obs}} \quad (7)$$

The bias-corrected annual time series of downscaled precipitation yielded in Equation (7) has the annual lag 1 auto correlations, the mean and the standard deviation of the observed precipitation.

Finally, the monthly time series of precipitation downscaled with GCM outputs were corrected using Equation (8).

$$Y_{i,j} = \frac{Z_j'''}{Z_j} \cdot Y_{i,j}''' \quad (8)$$

The future precipitation projections downscaled with GCM outputs were nested bias-corrected with the statistics of observed precipitation and precipitation downscaled with GCM outputs for the past climate, following the procedure described in Equations (3) to (8).

3.2.4. Potential of bias-correcting GCM outputs against reanalysis outputs

In this study, the precipitation downscaled with GCM outputs were bias-corrected against the observed precipitation. However, the bias-correction of each GCM output prior to its use on the downscaling model may seem to be a better option, as it removes the bias in each input variable of the downscaling model, individually. Although this method is computationally more expensive than the correction of bias in the precipitation downscaled from GCM outputs, it was important to verify whether the individual bias-correction of each GCM output is beneficial than its counterpart technique. In the absence of any readily available observations corresponding to the GCM outputs, the reanalysis outputs can be used as the reference for the bias-correction.

Instead of bias-correcting each GCM output against the corresponding reanalysis output, in this study, the benefit of this approach (if any) was deduced indirectly. For this purpose, the scatter of the precipitation output of the GCM, was plotted against the precipitation output of reanalysis data, for all four seasons. It is noteworthy to state here that the precipitation output of the GCM was identified as the most dominant potential predictor on the monthly observed precipitation, in the first article of this series. It was assumed that, the magnitudes of the scatter of the other GCM outputs used in the downscaling model were similar to that of the precipitation output of GCM.

Therefore, only the precipitation output of the GCM was considered in this analysis. Meanwhile, the scatter plots were also prepared for the precipitation downscaled with GCM outputs (before bias-correction) against the observed precipitation, for all seasons. Then the scatter of the precipitation downscaled with the outputs of the GCM (plotted against observed precipitation) was compared both visually and numerically with that of raw precipitation output of the GCM (plotted against reanalysis outputs). The numerical comparison of the magnitudes of the above described two scatter was performed considering the coefficient of determination (R^2).

Johnson and Sharma (2012) stated that, if the magnitude of the scatter of the variable to be bias-corrected is large (if large bias is present), then the bias-correction will not be effective. Therefore, it was understood that when the scatter of the raw outputs produced by the GCM is large, then the bias-correction of these GCM outputs prior to downscaling will not bring any additional advantage over the bias-correction of precipitation downscaled with the same GCM outputs.

4. Application

The generic methodology described in Section 3 was applied to the precipitation station at the Halls Gap post office in the operational area of GWMWater.

4.1. Reproduction of past precipitation and projection of precipitation into future with HadCM3 outputs

In this article, the downscaling model was run with both NCEP/NCAR reanalysis and HadCM3 20th century climate experiment data, for the reproduction of observed precipitation at the station of interest. The HadCM3 outputs were available at the spatial resolution of 2.75° latitude by 3.75° longitude. Owing to the mismatch of spatial resolutions between the NCEP/NCAR reanalysis outputs (2.5° latitude by 2.5° longitude) and HadCM3, the HadCM3 outputs were interpolated to the NCEP/NCAR grid (refer to Figure 1 in the first article of this series of articles) using the inverse distance weighted method (Ghosh and Mujumdar, 2008). The HadCM3 20th century climate experiment outputs for the period 1950–1999 were standardized with the means and the standard deviations of the corresponding NCEP/NCAR reanalysis outputs pertaining to the period 1950–1989 (calibration phase of this downscaling model) for each calendar month, before their application to the downscaling model. The means and the standard deviations of the NCEP/NCAR reanalysis output pertaining to the period 1950–1989 (calibration phase of the downscaling model) were treated as stationary components of the downscaling model. Figures 2 and 3 show the time series plots for the precipitation output of the downscaling model, with NCEP/NCAR and HadCM3 outputs respectively, over the period 1950–1999. The future precipitation projections were produced by introducing the HadCM3 outputs

corresponding to possible future climate, as inputs to the downscaling model, as described later in this article.

According to Figures 2 and 3, it was seen that, when the downscaling model developed with NCEP/NCAR outputs was run with HadCM3 outputs as inputs, it tended to overestimate the majority of precipitation compared to both observations and precipitation downscaled with NCEP/NCAR reanalysis outputs. This reflected the bias inherent in HadCM3 outputs with respect to that of NCEP/NCAR reanalysis outputs. The same finding was more clearly seen in scatter plot (b) of Figure 4. In scatter plot (a) of Figure 4, a good agreement between the precipitation downscaled with NCEP/NCAR outputs and the observations was seen (for more details refer to the first article). When the downscaling model was run with NCEP/NCAR outputs it displayed a Nash–Sutcliffe efficiency (NSE) (Nash and Sutcliffe, 1970) of 0.67 and a coefficient of determination (R^2) of 0.75. However, when the downscaling model was run with HadCM3 outputs those two statistics dropped to -0.62 and 0.12 , respectively.

Table 1 shows the performances of the downscaling model when run with NCEP/NCAR and HadCM3 outputs as inputs, in reproducing the observed monthly precipitation over the period 1950–1999. It also shows the statistics of the raw precipitation output of HadCM3 at grid point {4,4} of the atmospheric domain. It is noteworthy to state that the NCEP/NCAR reanalysis outputs are quality controlled and corrected against observations (Kalnay *et al.*, 1996). Since this downscaling model was calibrated and validated with NCEP/NCAR outputs, it inherently had an advantage in reproducing the observed precipitation better with NCEP/NCAR outputs, than that with HadCM3 outputs. The model was able to reproduce the average, the standard deviation and the coefficient of variation of observed precipitation with good accuracy in the period 1950–1999, when it was run with NCEP/NCAR reanalysis outputs. Also it displayed a Seasonally Adjusted Nash–Sutcliffe efficiency (SANS) (Wang, 2006; Sachindra *et al.*, 2013) of 0.79, resembling its good capabilities in reproducing observed precipitation. When the same model was run with HadCM3 outputs, it largely overpredicted the average of the precipitation. The standard deviation in the observations was properly captured by the model, when it was run with HadCM3 outputs. However, the performances of this model were limited according to the NSE, SANS and R^2 as shown in Table 1.

In Table 1, it was seen that raw precipitation output of HadCM3 severely underestimated the average and the standard deviation of the observed precipitation over the period 1950–1999. Also the SANS and the R^2 of the raw precipitation output of HadCM3 were quite low in comparison to those of precipitation reproduced by the downscaling with the outputs of HadCM3. Hence it was realized that the precipitation reproduced by the downscaling model with the outputs of HadCM3 are in better agreement with observations with respect to that of raw precipitation simulated by HadCM3.

4.2. Bias-correction

In this section, the application of the three bias-correction techniques to the precipitation downscaled with HadCM3 20th century climate experiment outputs is detailed. The precipitation downscaled with HadCM3 outputs was bias-corrected against the observed precipitation. The potential of bias-correcting raw outputs of HadCM3 against the corresponding NCEP/NCAR outputs are discussed at the end of this section.

4.2.1. Bias-correction of precipitation downscaled with HadCM3 outputs

EDQM, MBC and NBC (described in Section 3.2) were applied to the precipitation downscaled with the HadCM3 outputs. All bias corrections were performed over the 50-year period from 1950 to 1999, against the observed precipitation (considered as the reference precipitation for bias-correction) at the station of interest. Table 2(a) and b shows the season-based statistics of the observed precipitation and that reproduced by the downscaling model with NCEP/NCAR and HadCM3 outputs, before and after the application of the three bias-correction techniques. Table 2(a) refers to summer (December–February) and autumn (March–May), while Table 2(b) refers to winter (June–August) and spring (September–November). According to Table 2(a) and (b), it was seen that all three bias-correction techniques were capable in correcting the average of the precipitation downscaled with HadCM3 outputs adequately, in all four seasons. EDQM and MBC near-perfectly corrected the standard deviation in the precipitation reproduced with HadCM3 outputs, in all seasons. The NBC properly corrected the standard deviation of precipitation in summer and autumn, but an over estimation of it was seen in winter and spring. In NBC, initially the monthly lag 1 autocorrelations, the means and the standard deviations were corrected. This was followed by the correction of the annual lag 1 autocorrelations, the means and the standard deviations. Owing to this monthly to annual nesting procedure employed in NBC, slight distortions of monthly mean and standard deviation of precipitation could occur in some seasons. The coefficient of variations in the precipitation downscaled with HadCM3 were corrected by all three bias-correction techniques successfully, despite the slight over-estimation seen in winter and spring by NBC, which was due to the over-estimation of standard deviation described earlier. Overall, all three bias-correction techniques adequately corrected the average, the standard deviation and the coefficient of variation in all four seasons. Skewness of precipitation was well corrected in all four seasons by the EDQM technique. This is because, in EDQM, the CDF to be corrected is mapped onto the reference CDF, allowing all statistical moments to be matched. As described in subsections 3.2.2 and 3.2.3, in MBC and NBC, no explicit measure was taken to correct the skewness in precipitation. All bias-correction techniques were capable in improving the NSE of the precipitation reproduced with HadCM3 outputs in summer, autumn and winter.

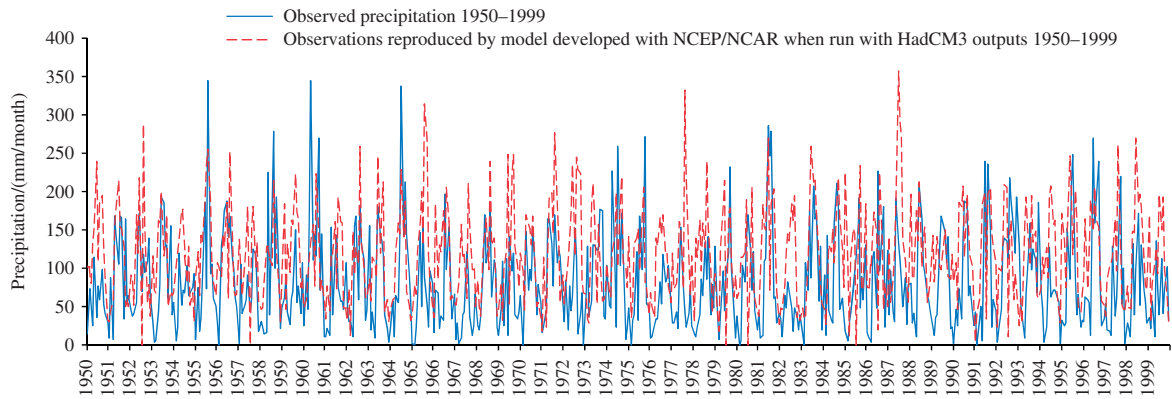


Figure 3. Time series plot for downscaling model run with HadCM3 outputs as inputs (1950–1999).

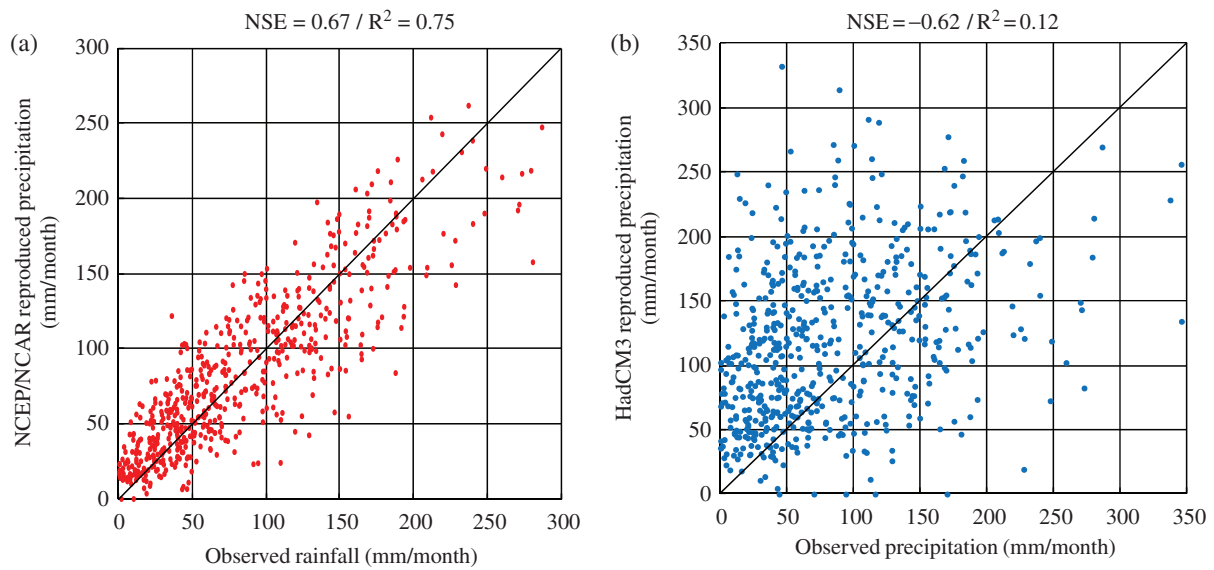


Figure 4. Scatter plots for downscaling model runs with (a) NCEP/NCAR and (b) HadCM3 outputs as inputs (1950–1999).

On the other hand, there was hardly any improvement to R^2 values of precipitation, after the bias-correction.

Figure 5 shows the seasonal scatter of the precipitation reproduced with HadCM3 outputs against the observed precipitation, before and after the application of three bias-correction methods. Before the application of the bias-corrections, during all four seasons, there was large scatter in precipitation, which mainly resembled an over-predicting trend. After each bias-correction, this large over-predicting trend reduced and it became a more balanced over and under-predicted scatter. In all four seasons, the scatter of precipitation after each bias-correction was visually similar to each other. However, the scatter which was seen prior to the bias-corrections did not shrink significantly after the application of any of the bias-correction techniques, in any of the four seasons. This is an indication that, these three bias-correction techniques hardly enhanced the accuracy of the time series of precipitation. Hence, it can be stated that when the scatter is very large as seen in Figure 5, the correction of the time series becomes difficult. However, all three bias-correction techniques were able to correct

the statistics of precipitation downscaled with HadCM3 outputs. Therefore, it was argued that the bias-corrected precipitation should be interpreted as a probabilistic prediction/projection, rather than from the point of view of a time series. For this purpose, EDQM was identified as the most suitable bias-correction technique as it preserves all statistical moments of the reference precipitation (in this study the observed precipitation for the period 1950–1999) for the past climate. Therefore, in this study, the EDQM was used for the bias-correction of future precipitation downscaled with HadCM3 outputs.

4.2.2. Validation of performances of EDQM technique

It is important to validate the performance of the EDQM technique prior to its use in the bias-correction of future precipitation projections. For this purpose, the statistics of the observed precipitation for the period 1950–1999 were compared with those of bias-corrected future precipitation downscaled with HadCM3 COMMIT emission scenario outputs for the period 2000–2099. The COMMIT is an idealized GHG emission scenario which assumes the GHG concentrations in the atmosphere at year 2000

Table 1. Performances of downscaling model with NCEP/NCAR and HadCM3 outputs.

Statistic	Period (1950–1999)			
	Observations	With NCEP/ NCAR outputs	With HadCM3 outputs	Raw HadCM3 Precipitation at grid point {4,4}
Avg	81.8	83.1	117.4	46.2
SD	62.2	53.8	61.8	28.4
C_v	0.76	0.65	0.52	0.61
NSE		0.67	−0.62	−0.27
SANS		0.79	0.26	−0.71
R^2		0.75	0.12	0.08

Avg = average of monthly precipitation in mm; SD = standard deviation of monthly precipitation in mm; C_v = coefficient of variation; SANS = seasonally adjusted Nash Sutcliffe efficiency; NSE = Nash–Sutcliffe efficiency; R^2 = coefficient of determination. Bold values refer to statistics of observed precipitation.

(CO₂ concentration in the atmosphere \approx 370 ppm) to be the same throughout the 21st century (Ojha *et al.*, 2010). Owing to the above attribute of the COMMIT emission scenario, it was assumed that it can closely characterize the climate simulated by HadCM3 in the latter half of the 20th century (1950–1999) during which the rise in the concentrations of GHGs was limited. In other words, a good agreement between the outputs of HadCM3 relevant to the 20th century climate experiment and for the COMMIT emission scenario was assumed. Furthermore, according to a study by Ojha *et al.* (2010), there is a close relation between the past observed precipitation and that statistically downscaled from the GCM outputs corresponding to the COMMIT scenario. Hence, in this study it was argued that if the statistics of the bias-corrected future precipitation downscaled from the HadCM3 COMMIT outputs were in close agreement with those of past observations, the EDQM technique has proven capabilities in bias-correcting future precipitation with adequate accuracy.

As a proof of the agreement between HadCM3 outputs of the 20th century climate experiment and those of COMMIT emission scenario, a comparison of the statistics of several potential predictors used in this study was performed. For this purpose, the HadCM3 simulated 1000 hPa specific humidity, 850 hPa relative humidity, 850 hPa zonal wind speed and precipitation corresponding to the 20th century climate experiment and the COMMIT emission scenario were interpolated to grid point {4,4} (refer to Figure 1 of the first article of this series of articles) using the inverse distance weighted method. Then the statistics of the above variables were computed for the 20th century climate experiment for the period 1950–1999 and also for the COMMIT emission scenario for the period 2000–2099. The comparison of these statistics of the potential predictors is shown in Table 3. In Table 3, it was seen that there is a very good agreement between the average, the standard deviation and the coefficient of variation of the potential variables simulated by HadCM3 under the 20th century climate experiment and the COMMIT emission scenario. It was assumed that, this is valid for all potential predictors used in this study.

For the validation of the performances of the EDQM technique, first the HadCM3 monthly outputs for the

COMMIT emission scenario pertaining to the period 2000–2099 were standardized with the monthly means and the standard deviations of the corresponding NCEP/NCAR reanalysis outputs, relevant to the period 1950–1989 (model calibration period). Then these standardized HadCM3 outputs for the COMMIT scenario were introduced to the downscaling model for projecting the monthly precipitation at the station of interest. For bias-correcting, observed precipitation for the period 1950–1999 was considered as the reference set of data, which is denoted by CDF1 in Figure 1. The CDF2 in the same figure refers to the precipitation downscaled with HadCM3 20th century climate experiment outputs for the same period. The future precipitation downscaled with HadCM3 COMMIT outputs for the period 2000–2099 was depicted by CDF3 in Figure 1. Following the EDQM procedure detailed in subsection 3.2.1, the future precipitation downscaled with HadCM3 outputs for the COMMIT scenario was bias-corrected. The statistics of the monthly precipitation downscaled with HadCM3 outputs for the COMMIT emission scenario before and after the bias-correction, for the future period 2000–2099, were compared with those of observed precipitation pertaining to the period 1950–1999, in Table 4(a) and (b). Table 4(a) refers to summer (December–February) and autumn (March–May), while Table 4(b) refers to winter (June–August) and spring (September–November). In Table 4(a) and (b), COMMIT (Before) and COMMIT (After) refer to the precipitation downscaled with HadCM3 COMMIT outputs, before and after the bias-correction, respectively.

As shown in Table 4(a) and (b), prior to the bias-correction, it was seen that the averages of the precipitation downscaled from HadCM3 COMMIT outputs were quite larger than those of observed precipitation, for all seasons. After the bias-correction, it was seen that the precipitation downscaled from HadCM3 COMMIT outputs, were able to reproduce the average of observed precipitation with good accuracy, in winter and spring. Despite some over-estimation, following the bias-correction, the averages of precipitation downscaled from COMMIT outputs for summer and autumn adequately agreed with those of observations. Before the bias-correction, except in autumn, the standard deviation of the precipitation

Table 2. Statistics of precipitation before and after bias-correction for (a) summer and autumn and (b) winter and spring.

Statistic	Summer (1950–1999)						Autumn (1950–1999)					
	Before bias-correction			After bias-correction			Before bias-correction			After bias-correction		
	Obs	With NCEP/NCAR outputs	With HadCM3 outputs	EDQM	MBC	NBC	Obs	With NCEP/NCAR outputs	With HadCM3 outputs	EDQM	MBC	NBC
Avg	41.4	44.3	73.6	41.5	44.8	41.4	70.4	70.7	117.7	70.4	70.9	68.0
SD	36.6	28.6	39.9	36.8	36.1	36.9	56.8	44.7	45.5	56.8	55.9	55.6
C_v	0.88	0.65	0.54	0.89	0.86	0.89	0.81	0.63	0.39	0.80	0.79	0.82
Skewness	1.62	1.34	1.28	1.63	1.57	1.94	1.36	0.70	-0.20	1.36	0.91	1.04
NSE	0.62	0.62	-0.41	0.13	0.18	0.16	0.71	0.71	0.64	0.69	0.70	0.69
R^2	0.52	0.52	0.01	0.02	0.03	0.03	0.65	0.65	0.09	0.04	0.04	0.03
Statistic	Winter (1950–1999)						Spring (1950–1999)					
	Before bias-correction			After bias-correction			Before bias-correction			After bias-correction		
	Obs	With NCEP/NCAR outputs	With HadCM3 outputs	EDQM	MBC	NBC	Obs	With NCEP/NCAR outputs	With HadCM3 outputs	EDQM	MBC	NBC
Avg	127.3	128.7	164.5	126.9	127.5	126.3	88.1	88.7	113.9	88.1	88.3	87.6
SD	64.8	55.7	68.2	65.2	64.4	75.2	53.7	43.7	53.4	53.7	53.4	60.4
C_v	0.51	0.43	0.41	0.51	0.50	0.59	0.61	0.49	0.47	0.61	0.60	0.69
Skewness	0.76	0.39	-0.20	0.73	0.55	0.87	1.09	0.99	0.65	1.09	0.82	1.11
NSE	0.85	0.85	0.11	0.32	0.34	0.23	0.80	0.80	-0.73	-0.85	-0.82	-1.15
R^2	0.72	0.72	0.00	0.01	0.01	0.01	0.69	0.69	0.03	0.00	0.00	0.00

Avg = average of monthly precipitation in mm; SD = standard deviation of monthly precipitation in mm; C_v = coefficient of variation; Skewness = (Avg - Mode)/SD; NSE = Nash-Sutcliffe efficiency; R^2 = coefficient of determination; Obs = observed monthly precipitation; EDQM = equidistant quantile mapping; MBC = monthly bias-correction; NBC = nested bias-correction. Bold values refer to statistics of observed precipitation.

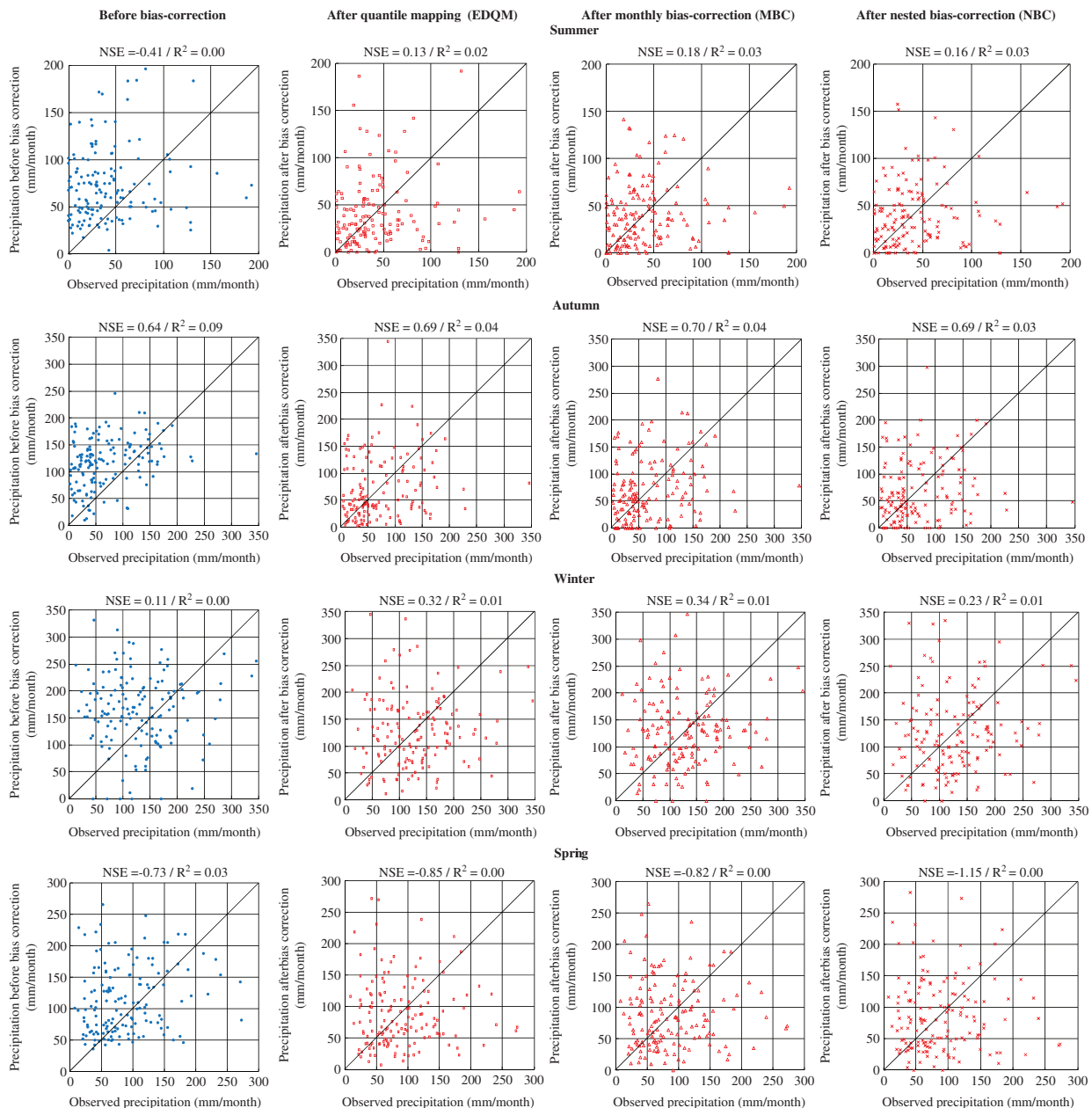


Figure 5. Seasonal scatter plots for precipitation downscaled with HadCM3 outputs, before and after bias-correction (1950–1999).

downscaled with HadCM3 COMMIT outputs displayed an over-predicting trend. Even after the bias-correction this trend was evident in all seasons.

In this study, empirical distribution functions of the observed precipitation and precipitation downscaled from HadCM3 outputs were used in applying the EDQM technique. This raised the need of frequent interpolation and extrapolation of the CDFs of observed precipitation and that downscaled with HadCM3 20th century climate experiment outputs. This procedure increases the severity of low and high extreme precipitation. The over-prediction of the maximum monthly precipitation was due to the extrapolation of the above CDFs and it can be minimized by fitting suitable theoretical distribution functions to the observed and downscaled precipitation time series, prior to the application of the EDQM technique

(Li *et al.*, 2010). However, it should be noted that when a theoretical distribution function is fitted to a dataset, inevitably, there will be fitting errors as no theoretical distribution function can perfectly describe any precipitation dataset.

Before the bias-correction, the 10th, 25th, 50th, 75th and 90th percentiles of the downscaled precipitation for COMMIT scenario were largely over-estimated, in all seasons. After the bias-correction, in all seasons, the over-estimating characteristic of the above percentiles of precipitation downscaled with HadCM3 COMMIT outputs reduced. In all four seasons, the percentages of months with zero precipitation were over-estimated. However, this trend was minimal in summer. After the bias-correction, the percentages of months with above average

Table 3. Comparison of statistics of potential predictors between the 20th century climate experiment and the COMMIT scenario.

Statistic	Precipitation (mm)		1000 hPa Specific humidity (grams kg ⁻¹)		850 hPa Relative humidity (%)		850 hPa Zonal wind speed (m s ⁻¹)	
	20C3M	COMMIT	20C3M	COMMIT	20C3M	COMMIT	20C3M	COMMIT
	1950–1999	2000–2099	1950–1999	2000–2099	1950–1999	2000–2099	1950–1999	2000–2099
Avg	47.9	45.2	7.2	7.7	63.7	63.8	4.2	4.2
SD	30.4	27.5	1.0	1.1	9.6	9.4	3.2	3.3
C _v	0.63	0.61	0.14	0.14	0.15	0.15	0.75	0.79

Avg = average; SD = standard deviation; C_v = coefficient of variation; 20C3M = 20th century climate experiment; COMMIT = COMMIT emission scenario.

precipitation under the COMMIT scenario matched with those of observations, in all seasons acceptably.

4.2.3. Potential of bias-correcting HadCM3 outputs against NCEP/NCAR outputs

Although the bias was prevalent in the HadCM3 outputs (as shown in the first article of this series of articles), in this study, the bias-correction was performed on the precipitation downscaled with the HadCM3 outputs. This method was employed as it was computationally much cheaper than bias-correcting each output of HadCM3 individually, prior to their use in downscaling. However, theoretically, the bias-correction of each GCM output individually, before introducing to a downscaling model seems to be a more effective approach than the correction of bias in the precipitation downscaled with raw GCM outputs. In the absence of any readily available observations corresponding to the GCM outputs used in the downscaling model, the bias-correction of these GCM outputs can be performed against the pertaining NCEP/NCAR or any other reanalysis outputs (e.g. Salvi *et al.*, 2011).

According to Figure 5, it was seen that if the scatter of the variable to be bias-corrected (e.g. precipitation downscaled with GCM outputs) was large, none of the bias-correction techniques used in this study was capable in adequately reducing this scatter. If the scatter was not adequately reduced, the time series of the variable is also not properly corrected. Based on this argument, it was decided to visualize the raw precipitation output of HadCM3 against that of NCEP/NCAR in scatter plots, pertaining to grid point {4,4} (refer to Figure 1 in the first article, for the location of this grid point), for each season. The grid point {4,4} referred to the point which was located closest to the precipitation station considered in this study. In the first article, precipitation output of HadCM3 at grid point {4,4} was identified as the most influential potential variable on the observed monthly precipitation.

Figure 6 shows the scatter plots of raw precipitation output of HadCM3 against that of NCEP/NCAR for the period 1950–1999, corresponding to grid point {4,4}. As shown in Figure 6, it is realized that there is large scatter in the raw precipitation outputs of HadCM3 in all four seasons. The very low R² values in all seasons numerically verified the presence of large scatter in precipitation

outputs of HadCM3. It is also reasonable to assume that, such large scatter is prevalent in the other outputs of HadCM3 which were used in the downscaling model, since all these outputs were produced by the same GCM. Therefore, it was deduced that if the HadCM3 outputs were bias-corrected against the NCEP/NCAR reanalysis outputs with any of the bias-correction techniques used in this study, the improvement to their time series will be minimal. Without considerable improvement to the time series of HadCM3 outputs, it was difficult to expect any improvement to the precipitation downscaled with these individually bias-corrected HadCM3 outputs. Hence, the bias-correction of outputs of HadCM3, prior to downscaling, was identified as a procedure which brings no additional advantage.

4.3. Future precipitation projections

4.3.1. Greenhouse gas emission scenarios

For this study, two GHG emission scenarios namely; A2 and B1 were selected. A2 is a relatively high GHG emission scenario due to its economic focus. On the other hand, the B1 GHG emission scenario described a world with high level of concern on the environment and sustainable development. Therefore, it refers to relatively low level of GHG emissions. The A2 and B1 GHG emission scenarios referred to carbon dioxide concentrations of about 850 ppm and 550 ppm, respectively, by the end of the 21st century (IPCC, 2000). The downscaling model was used to project the future precipitation at the station of interest, up to year 2099. HadCM3 outputs for the A2 and B1 GHG emission scenarios of the IPCC were obtained from the PCMDI website (<https://esgcat.llnl.gov:8443/index.jsp>), for the period 2000–2099, and used as the inputs to the downscaling model used in this study.

4.3.2. Bias-corrected future precipitation projections

HadCM3 outputs for the A2 and B1 IPCC SRES GHG emission scenarios for the period 2000–2099 were standardized with the means and the standard deviations of the corresponding NCEP/NCAR reanalysis outputs, pertaining to the model calibration period which spanned over 1950–1989. Thereafter, these standardized HadCM3 outputs were introduced to the downscaling model. This allowed the monthly precipitation projections at the

Table 4. Seasonal statistics of observed and COMMIT precipitation for (a) summer and autumn and (b) winter and spring.

(a)	Summer			Autumn		
	1950–1999	2000–2099		1950–1999	2000–2099	
	Obs	COMMIT (Before)	COMMIT (After)	Obs	COMMIT (Before)	COMMIT (After)
Avg	41.4	<i>87.6</i>	55.6	70.4	<i>124.9</i>	78.7
SD	36.6	<i>57.4</i>	51.1	56.8	<i>51.0</i>	65
C_v	0.88	<i>0.65</i>	0.92	0.81	<i>0.41</i>	0.83
Minimum precipitation	0.0	<i>14.2</i>	0.0	2.8	<i>10.1</i>	0.0
Maximum precipitation	192.3	<i>347.0</i>	301	345.4	<i>271.0</i>	385
10th Percentile	4.2	<i>34.6</i>	5.3	11.4	<i>55.1</i>	13.6
25th Percentile	16.4	<i>46.7</i>	18.0	30.1	<i>82.7</i>	29.0
50th Percentile	30.7	<i>68.7</i>	45.1	49.1	<i>130.5</i>	61.4
75th Percentile	54.9	<i>112.6</i>	82.3	108.6	<i>161.1</i>	122.9
90th Percentile	90.7	<i>159.3</i>	114.9	148.7	<i>187.4</i>	168.1
Percentage of months with zero precipitation	4	<i>0</i>	6	0	<i>0</i>	6
Percentage of months with above average precipitation	39	<i>38</i>	37	39	<i>53</i>	41

(b)	Winter			Spring		
	1950–1999	2000–2099		1950–1999	2000–2099	
	Obs	COMMIT (Before)	COMMIT (After)	Obs	COMMIT (Before)	COMMIT (After)
Avg	127.3	<i>161.1</i>	124.3	88.1	<i>116.7</i>	91.5
SD	64.8	<i>72.9</i>	71.5	53.7	<i>67.3</i>	71.6
C_v	0.51	<i>0.45</i>	0.58	0.61	<i>0.58</i>	0.78
Minimum precipitation	12.2	<i>2.0</i>	0.0	7.6	<i>23.1</i>	0.0
Maximum precipitation	345.2	<i>387.5</i>	424.1	272.4	<i>321.6</i>	346.5
10th Percentile	47.8	<i>63.1</i>	41.4	31.4	<i>48.4</i>	17.4
25th Percentile	77.4	<i>109.0</i>	73.2	48.7	<i>63.2</i>	41.5
50th Percentile	119.3	<i>163.1</i>	118.2	73	<i>95.7</i>	67.9
75th Percentile	167.6	<i>208.5</i>	170.8	118.8	<i>156.8</i>	125.0
90th Percentile	207.7	<i>254.9</i>	202.5	156.1	<i>218.2</i>	198.6
Percentage of months with zero precipitation	0	<i>0</i>	5	0	<i>0</i>	3
Percentage of months with above average precipitation	47	<i>51</i>	47	43	<i>40</i>	41

Avg = average of monthly precipitation in mm; SD = standard deviation of monthly precipitation in mm; C_v = coefficient of variation; COMMIT (Before) = Precipitation downscaled for COMMIT scenario before bias-correction (italicized values); COMMIT (After) = Precipitation downscaled for COMMIT scenario after bias-correction. Bold values refer to statistics of observations.

station of interest up to year 2099. The precipitation projections under A2 and B1 emission scenarios by the downscaling model were bias-corrected using the EDQM technique, as detailed in subsection 3.2.1.

In Table 5, the statistics of the future precipitation projections for the period 2000–2099 are shown against those of observed precipitation for the period 1950–1999. The percentage changes in the statistics of the future precipitation projections with respect to the statistics of observed precipitation of the period 1950–1999 are also provided within parentheses in Table 5. According to Table 5, at the station of interest, in summer and spring, the average of monthly precipitation for the period 2000–2099 showed a decline under both A2 and B1 emission scenarios. On the other hand, in winter, both

A2 and B1 emission scenarios indicated a rise in the average of monthly precipitation. During autumn, only A2 emission scenario showed a rise in the average of the monthly precipitation. The standard deviation of the precipitation under both A2 and B1 scenarios increased in all seasons in comparison to that of observations corresponding to the period 1950–1999. The two sample *t*-test revealed that the changes in the average of future precipitation in autumn and winter under both A2 and B1 scenarios are not significant at the 95% confidence level. However, it was found that the decrease in the average of precipitation projected into future in spring was significant at the 95% confidence level for both GHG emission scenarios. Furthermore, the two sample *F*-test revealed that the rise in the standard deviation of the precipitation

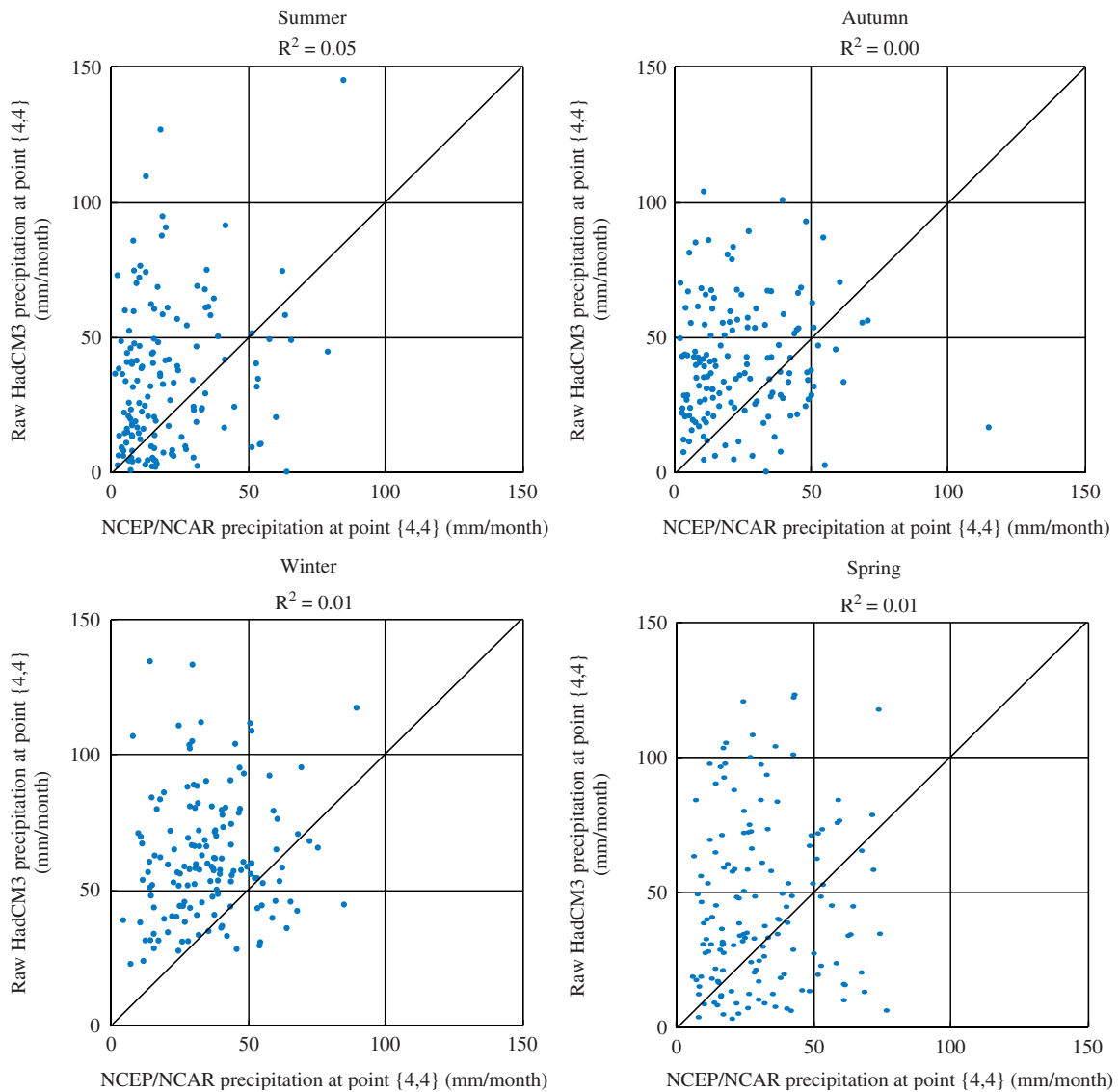


Figure 6. Seasonal scatter plots for raw precipitation output of HadCM3 at point {4,4} (1950–1999).

projected into future compared to that of observed precipitation of period 1950–1999 was statistically significant at the 95% confidence level for both A2 and B1 emission scenarios in all seasons except in winter.

In summer and winter, the precipitation in Victoria is influenced by the strength and the location of the sub-tropical ridge (<http://www.climatekelpie.com.au/understand-climate/weather-and-climate-drivers/victoria#SubtropicalRidge>). In summer, the sub-tropical ridge mainly lies over the southern part of the Australian continent (latitude 40°S – Timbal and Drosdowsky 2013). In winter, it is located over the north central region of Australia (latitude 29°S – Timbal and Drosdowsky 2013). The increase in the GHG emissions causes the atmospheric temperature to rise and this leads to strengthening (rise in pressure) and the southward movement of the sub-tropical ridge (Commonwealth Scientific and Industrial Research Organisation, 2010). This phenomenon can cause a decrease in precipitation in summer and winter as the pressure in the sub-tropical ridge is high. The

relatively larger rise in the GHG emissions characterized by A2 scenario can intensify the sub-tropical ridge and cause relatively larger drop in the average of the precipitation in comparison to the same caused by B1 scenario which is associated with relatively low emissions in summer and winter, as shown in Table 5.

In all four seasons, both A2 and B1 scenarios depicted an increase in the maximum monthly precipitation, in comparison with that of past observations. This rise was particularly higher under A2 emission scenario which was associated with relatively higher levels of GHG emissions. This indicated that in future, with the rising GHG levels in the atmosphere, there will be months with large precipitation totals, at the station of interest. However, it should be noted that high monthly precipitations are prone to extrapolation errors of CDFs, as stated previously in the validation of the performances of the EDQM technique. The MLR technique used in developing the downscaling model employed in this study can only determine the linear component of the relationships

Table 5. Seasonal statistics of future A2 and B1 bias-corrected precipitation.

Statistic	Summer			Autumn			Winter			Spring		
	2000–2099		1950–1999	2000–2099		1950–1999	2000–2099		1950–1999	2000–2099		
	A2	B1	Obs	A2	B1	Obs	A2	B1	Obs	A2	B1	
Avg	33.6 (-19%↓)*	35.3 (-15%↓)^	41.4	76.8 (+9%↑)^	67.6 (-4%↓)^	127.3	132.2 (+4%↑)^	135.6 (+7%↑)^	88.1	74.5 (-15%↓)*	71.0 (-19%↓)*	
SD	44.0 (+20%↑)*	43.1 (+18%↑)*	36.6	65.5 (+15%↑)*	66.8 (+18%↑)*	64.8	72.0 (+11%↑)^	73.4 (+13%↑)*	53.7	69.2 (+29%↑)*	63.1 (+18%↑)*	
Maximum precipitation	376.4 (+96%↑)	251.9 (+31%↑)	192.3	424.2 (+23%↑)	418.5 (+21%↑)	345.2	527.4 (+53%↑)	494.1 (+43%↑)	272.4	383.8 (+41%↑)	319.9 (+17%↑)	
Percentage of months with zero precipitation	20 (+16%↑)	24 (+20%↑)	4	6 (+6%↑)	10 (+10%↑)	0	1 (+1%↑)	0 (0% =)	0	8 (+8%↑)	5 (+5%↑)	
Percentage of months with above average precipitation	31 (-8%↓)	37 (-2%↓)	39	40 (+1%↑)	39 (0% =)	47	46 (-1%↓)	48 (+1%↑)	43	39 (-4%↓)	38 (-5%↓)	

Avg = average of monthly precipitation in mm; SD = standard deviation of monthly precipitation in mm; C_v = coefficient of variation; A2 = high emission scenario; B1 = low emission scenario; ↑ = percentage increase in 2000–2099 with respect to observations of period 1950–1999; ↓ = percentage decrease in 2000–2099 with respect to observations of period 1950–1999 (in bold); Symbol = indicates change in percentage in 2000–2099 with respect to observations of period 1950–1999 (in italics); Symbol * indicates statistically significant change at 95% confidence level; Symbol ^ statistically insignificant change at 95% confidence level.

between the predictors and the precipitation. High values of precipitation usually display nonlinear relationships with predictors. Therefore the downscaling technique used in this study can be regarded as another source of uncertainty in the simulations of high precipitation values.

In all four seasons, the A2 scenario projected a rise in the percentage of months with zero precipitations, indicating that there will be greater number of dryer months in future, with increasing GHG emissions. A similar trend was seen in the projected precipitation pertaining to the B1 scenario, except in winter, when no months with zero precipitation was seen. It is noteworthy to state that the rise in the percentage of months with zero precipitation was highest in summer, for both A2 and B1 emission scenarios. In winter, the rise in the percentage of zero precipitation months was relatively low, in comparison with that of rest of the seasons, for the A2 emission scenario. In summer and spring both A2 and B1 emission scenarios indicated a slight decrease in the percentage of months with above average precipitation. In autumn and winter the changes in the percentage of months with above average precipitation was negligible for both emission scenarios.

A comparison conducted between the statistics of the raw precipitation outputs of HadCM3 corresponding to A2 and B1 GHG emission scenarios of the period 2000–2099, revealed that the differences between the averages and the standard deviations of precipitation at point {4,4} of the atmospheric domain were quite negligible in all seasons. However, the maximum of monthly precipitation simulated by HadCM3 under A2 scenario was clearly higher than that under B1 scenario in all seasons. This indicated that the relative changes in the GHG concentrations characterized by the A2 and B1 scenarios do not cause a significant difference in the long-term average and the standard deviation of precipitation simulated by HadCM3 over the study area, but the high emissions associated with A2 scenario causes HadCM3 to simulate peak precipitation values higher than those simulated with B1 scenario in all seasons. Similar characteristics are seen in the statistics of precipitation in Table 5 down-scaled using the HadCM3 outputs pertaining to A2 and B1 scenarios. When the atmospheric GHG concentration rises, it causes an imbalance in radiative energy which increases the heat energy stored in the sea leading to an elevation in the sea surface temperatures (Trenberth *et al.*, 2007). The rise in the sea surface temperature increases the rate of evaporation, hence the water vapour content in the atmosphere. These phenomena lead to intensification of the hydrologic cycle causing a rise in the magnitude of the maximum precipitation (Kunkel *et al.*, 2013). Since the GHG emissions associated with the A2 scenario are higher in comparison to those of B1, the rise in the magnitude of the maximum precipitation is higher for A2 in all seasons as shown in Table 5.

Figure 7 depicts the exceedance curves for future A2 and B1 bias-corrected monthly precipitation for the period 2000–2099, along with the exceedance curves for the observed monthly precipitation pertaining to the period 1950–1999. According to Figure 7, it is evident that the precipitation in autumn and winter will increase with respect to the observations of the period 1950–1999, for the majority of exceedance probabilities. However, in spring there will be a drop in precipitation pertaining to the majority exceedance probabilities, and in summer a relatively small decrease in precipitation was indicated for most of the exceedance probabilities. These findings are also consistent with the numerical assessments provided in Table 5.

Smith and Chandler (2009) stated that, over the Murray Darling basin (MDB) in south east Australia, the raw precipitation output of HadCM3 under the A1B emission scenario (mid-level scenario which refers to an atmospheric CO₂ concentration of about 720 ppm at the end of the 21st century) shows a decrease in precipitation of about 15% for the period 2071–2099, with respect to the observed precipitation in the period 1971–2000. According to the findings of this study, at the Halls Gap post office which is located close to the southern boundary of the MDB (within it), the precipitation downscaled with HadCM3 outputs pertaining to A2 and B1 scenarios for the period 2071–2099, showed decrease of about 12% and 3.4%, respectively, with respect to the observed precipitation in the period 1971–2000. The Victorian Government Department of Sustainability and Environment (2008) stated that the median estimates obtained from the raw precipitation outputs of number of GCMs under B1 (low emissions), and A1F1 (high emissions) emission scenarios have indicated a drop in the average of precipitation in all four seasons by the year 2070 over the Wimmera region, which included the Halls Gap post office. Furthermore, it was stated that the greatest reduction in precipitation is likely to occur in spring, which is consistent with the findings of this study. Also it was stated that the intensity of extreme daily precipitation is likely to increase in the Wimmera region. However, it should be noted that there were no evidence in the literature of previous attempts on statistical downscaling of GCM outputs to precipitation at Halls Gap or its surrounding area. Future climate information for water resource planning purposes in the study area is currently based on the regional estimates derived from the raw outputs of GCMs (e.g. Commonwealth Scientific and Industrial Research Organisation, 2007) and does not provide the spatial resolution of detail that will be needed at the catchment scale.

The long-term statistics of monthly precipitation such as average, variance, extremes, and so on, extracted from the bias-corrected time series of monthly precipitation are useful for water resource planning purposes. The average of the future precipitation enables the understanding of the future water availability in a catchment, in meeting the future demand. The variance

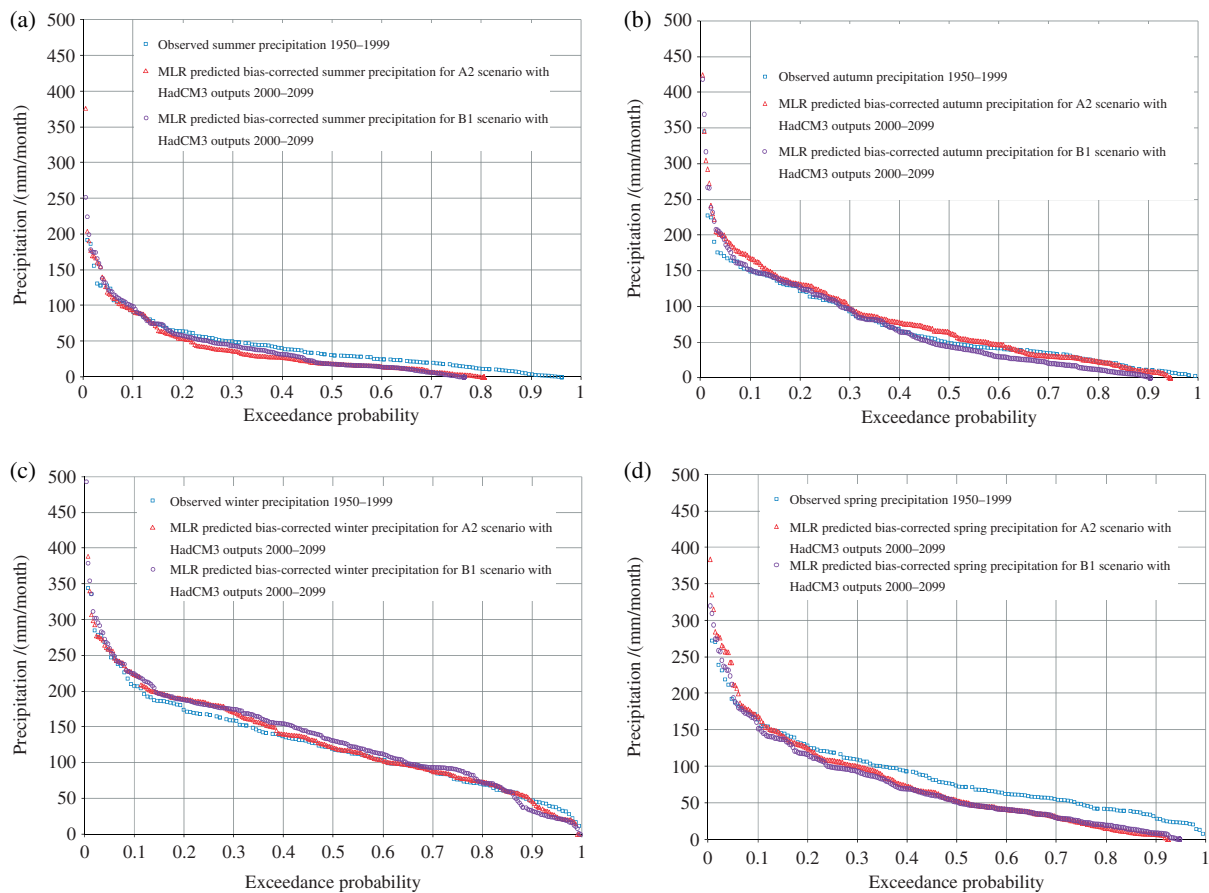


Figure 7. Seasonal exceedance curves for future bias-corrected precipitation under A2 and B1 emission scenarios (2000–2099). (a) Summer, (b) autumn, (c) winter and (d) spring.

of precipitation describes the amount of change in precipitation with respect to its average. A larger variance in future precipitation at the catchment scale shows unique challenges in managing water resources to withstand the larger fluctuations in precipitation. Greater variation in future precipitation will need to be considered in the planning and operation of water resources infrastructure, and will impact on the reliability of supply to customers. Modelling extreme low and high precipitation values are important in the management of droughts and floods, respectively.

Owing to the downscaling of GCM outputs followed by the bias-correction of downscaled precipitation, this research provides useful, area-specific information to the water resource planners (in the study area), than the currently available future climatic information derived from raw GCM outputs. In future, the methodology described in this article will be applied to a number of sites in the operational area of GWMWater (refer to Figure 1 of the first article) for producing the future precipitation projections with the outputs of multiple GCMs.

4.3.3. Caveats and uncertainties involved in the study

Statistical downscaling is a useful tool for the determination of catchment scale hydroclimatology using the GCM

outputs. However, the projections produced using statistical downscaling techniques are subject to uncertainties arising from many sources such as GHG emission scenarios, GCMs, observations of predictands against which the downscaling models are calibrated and also from the downscaling techniques used (Hashmi *et al.*, 2009). The largest uncertainty in a downscaling study often arises from the GHG emission scenarios. This is because the actual levels of GHG emissions pertaining to the future climate are not known at the time the climate projections are produced. In this study, A2 which is a high emission scenario and B1 which is a low emission scenario were used for the projection of precipitation into future. Therefore, the statistics of precipitation derived from the outputs of the downscaling model refer to two plausible climate states conditioned by high and low GHG emission levels. Hence the precipitation projections produced in this study should not be treated as definite but as plausible.

Mainly owing to the different assumptions and approximations employed in the structure, different GCMs may tend to produce different projections of the future climate (Yu *et al.*, 2002) even under the same GHG emission scenario. This causes the downscaling models fed with the outputs of different GCMs to simulate future climate over the same study area differently. The above effect due to

the use of different GCMs is particularly evident when the predictors used as inputs to the downscaling models have a low degree of convergence among different GCMs. Johnson and Sharma (2009) found that GCMs show relatively high convergence for pressure and surface air temperature and comparably low convergence for precipitation, over Australia under both A2 and B1 GHG emission scenarios. This indicated that if the precipitation outputs of different GCMs are used as inputs to a downscaling model, it will probably tend to produce different projections of precipitation at the catchment scale. In this study, precipitation simulated by HadCM3 was used as an input to 11 of the 12 calendar month-based downscaling models, for the projection of precipitation into future. Therefore, the downscaling model used in this study will tend to produce a range of catchment scale projections of precipitation when run with the outputs of different GCMs. It should be noted that the statistics of the precipitation projected into future in this study correspond to the future climate simulated by HadCM3. By using the outputs of different GCMs and hence obtaining the ensemble average projection for precipitation can reduce the dependence on one specific GCM.

The uncertainties rising from the observations of precipitation also can cause the downscaling model to be less robust. In this study, the daily precipitation data were used to derive the monthly precipitation needed for the model calibration and validation and also for the correction of bias in the precipitation simulated by the downscaling model. The daily observed precipitation record at the Halls Gap post office contained 31% missing data over the period 1950–2010. These missing data have been filled by the Queensland Climate Change Centre of Excellence in the SILO database, using the spatial interpolation method described by Jeffrey *et al.* (2001). Since about one third of the daily precipitation observations were estimated, the record of observations at the Halls Gap post office may have introduced uncertainties to the downscaling model and also to the bias-correction.

Another possible source of uncertainty in a downscaling exercise is the downscaling technique used for deriving the relationship between the predictors and the predictand. In this study, MLR which is a linear regression technique was employed for the above purpose. Though MLR is a simple and convenient technique for developing a downscaling model, it cannot capture the nonlinear component of the relationships between the predictors and precipitation. Theoretically a complex nonlinear regression technique such as SVM or ANN could be able to better capture the relationships between the predictors and precipitation. However, the improvement to the simulations produced by such downscaling model built using a complex nonlinear regression technique over a downscaling model developed with a relatively simpler linear regression method may depend upon the degree of nonlinearity in the relationships between the predictors and the predictand.

5. Summary and conclusions

In the first article of this series of two articles, two models were developed using the MLR technique for downscaling NCEP/NCAR and HadCM3 outputs to monthly precipitation. In that study, it was realized that the model built with NCEP/NCAR outputs performed better than the model that was developed with HadCM3 outputs. The large mismatch seen between the raw precipitation output of HadCM3 and the observed precipitation in the first article, showed the need of a bias-correction. In this study the model built with NCEP/NCAR outputs (which is referred to as 'the downscaling model' throughout this article) was used for the future projections of monthly precipitation at the Halls Gap post office located in north western Victoria, Australia, with HadCM3 outputs corresponding to possible future climate as inputs. Also a bias-correction to the precipitation downscaled with HadCM3 outputs was performed.

The HadCM3 outputs for the 20th century climate experiment for the period 1950–1999 were standardized with the means and standard deviations of NCEP/NCAR reanalysis outputs corresponding to the period 1950–1989 (this was the calibration period of the downscaling model). Then these standardized HadCM3 outputs were introduced to the downscaling model for reproducing the observed monthly precipitation from 1950 to 1999, for the precipitation station at the Halls Gap post office. The precipitation downscaled with HadCM3 20th century climate experiment outputs were bias-corrected against the observed precipitation relevant to the period 1950–1999. The bias-correction of precipitation was performed using three different techniques: (1) EDQM, (2) MBC and (3) NBC. Each of these techniques were applied separately on the monthly precipitation downscaled with HadCM3 outputs on each calendar month. Based on the performances, the EDQM technique was identified as the most suitable method for correcting the bias in precipitation downscaled with HadCM3 outputs. The performances of the EDQM technique was validated by comparing the statistics of the precipitation downscaled with HadCM3 outputs pertaining to the COMMIT emission scenario for the period 2000–2099, with those of observed precipitation for the period 1950–1999.

HadCM3 outputs for the future climate were obtained under the A2 and B1 greenhouse emission scenarios for the projection of monthly precipitation into future. The A2 and B1 HadCM3 outputs for the period 2000–2099 were standardized with the means and standard deviations of NCEP/NCAR reanalysis outputs pertaining to the period 1950–1989. These standardized outputs of HadCM3 for the A2 and B1 emission scenarios were applied on the downscaling model for producing the future precipitation at the Halls Gap post office. The future precipitation downscaled from HadCM3 outputs corresponding to A2 and B1 emission scenarios were bias-corrected against the observed precipitation, using the EDQM technique.

The conclusions drawn from this study are:

1. When the downscaling model developed with NCEP/NCAR reanalysis data was run with HadCM3 20th century climate experiment outputs for the period 1950–1999, the model largely over-estimated the majority of monthly precipitation. There was large scatter in precipitation reproduced with HadCM3 outputs, during all four seasons.
2. After the application of EDQM, monthly bias-correction and NBC techniques for the period 1950–1999, the large over-predicting trend of precipitation reduced and turned into a more balanced over and under-predicted scatter. However, none of the bias-correction techniques could satisfactorily reduce the scatter of monthly precipitation.
3. Considering the scatter that was present in precipitation after the bias-correction, it was seen that all three bias-correction techniques hardly enhanced the accuracy of the time series of monthly precipitation.
4. In all seasons, during the period 1950–1999, EDQM, MBC and NBC techniques adequately corrected the average, the standard deviation and the coefficient of variation of monthly precipitation.
5. Following (3) and (4), it was argued that the bias-corrected precipitation should produce probability distributions of the projections more accurately than the time series.
6. For the bias-correction of monthly precipitation, EDQM was identified as the most suitable technique, employed in this study, as this method was the best in correcting the cumulative distribution (and hence the probability distribution) of the precipitation down-scaled with GCM outputs. EDQM has a sound theory to model the CDF accurately.
7. If the scatter of the raw GCM outputs against NCEP/NCAR outputs was large, it was understood that the bias-correction of raw outputs of a GCM against NCEP/NCAR outputs prior to downscaling is not advantageous, than the bias-correction of the predictand (e.g. precipitation) downscaled from the same set of raw GCM outputs.
8. For the period 2000–2099, in spring, the precipitation downscaled using HadCM3 outputs pertaining to both A2 (relatively high emissions) and B1 (relatively low emissions) scenarios showed a statistically significant (at 95% confidence level) decrease in the average of monthly precipitation with respect to the average of observed precipitation of the period 1950–1999.

Acknowledgements

The authors acknowledge the financial assistance provided by the Australian Research Council Linkage Grant scheme and the Grampians Wimmera Mallee Water Corporation for this project. The authors also wish to thank the editor and the two anonymous reviewers for their useful comments, which have improved the quality of this article.

References

- Arnell NW, Gosling SN. 2013. The impacts of climate change on river flow regimes at the global scale. *J. Hydrol.* **486**: 351–364, DOI: 10.1016/j.jhydrol.2013.02.010.
- Charles A, Timbal B, Fernandez E, Hendon H. 2013. Analog downscaling of seasonal rainfall forecasts in the Murray Darling basin. *Mon. Weather Rev.* **141**: 1099–1117, DOI: 10.1175/MWR-D-12-00098.1.
- Chen C, Haerter JO, Hagemann S, Piani C. 2011. On the contribution of statistical bias correction to the uncertainty in the projected hydrological cycle. *Geophys. Res. Lett.* **38**: 1–6, DOI: 10.1029/2011GL049318.
- Chen J, Brissette FP, Leconte R. 2012. Downscaling of weather generator parameters to quantify hydrological impacts of climate change. *Clim. Res.* **51**: 185–200, DOI: 10.3354/cr01062.
- Chu JT, Xia J, Xu CY, Singh VP. 2010. Statistical downscaling of daily mean temperature, pan evaporation and precipitation for climate change scenarios in Haihe River, China. *Theor. Appl. Climatol.* **99**: 149–161, DOI: 10.1007/s00704-009-0129-6.
- Commonwealth Scientific and Industrial Research Organisation. 2007. *Wimmera Region Fact Sheet: Murray-Darling Basin Sustainable Yields Project*. Retrieved October 28, 2012. <http://www.csiro.au/Outcomes/Water/Water-for-the-environment/Wimmera-region-fact-sheet-Murray-Darling-Basin-Sustainable-Yields-Project.aspx>
- Commonwealth Scientific and Industrial Research Organisation. 2010. *Climate Variability and Change in South-Eastern Australia: A Synthesis of Findings from Phase 1 of the South Eastern Australian Climate Initiative (SEACI)*. Retrieved July 17, 2013. http://www.seaci.org/publications/documents/SEACI-1%20Reports/Phase1_SynthesisReport.pdf
- Dessai S, Lu X, Hulme M. 2005. Limited sensitivity analysis of regional climate change probabilities for the 21st century. *J. Geophys. Res. D: Atmos.* **110**: 1–17, DOI: 10.1029/2005JD005919.
- Earth System Research Laboratory. 2013. *Trends in Atmospheric Carbon Dioxide*. Retrieved June 20, 2013. <http://www.esrl.noaa.gov/gmd/ccgg/trends/global.html>
- Fatichi S, Ivanov VY, Caporali E. 2011. Simulation of future climate scenarios with a weather generator. *Adv. Water Resour.* **34**: 448–467, DOI: 10.1016/j.advwatres.2010.12.013.
- Fu G, Charles SP, Kirshner S. 2012. Daily rainfall projections from general circulation models with a downscaling nonhomogeneous hidden Markov model (NHMM) for south-eastern Australia. *Hydrol. Process.* **27**: 3663–3673, DOI: 10.1002/hyp.9483.
- Ghosh S, Katkar S. 2012. Modeling uncertainty resulting from multiple downscaling methods in assessing hydrological impacts of climate change. *Water Resour. Manage.* **26**: 3559–3579, DOI: 10.1007/s11269-012-0090-5.
- Ghosh S, Mujumdar PP. 2008. Statistical downscaling of GCM simulations to streamflow using relevance vector machine. *Adv. Water Resour.* **31**: 132–146, DOI: 10.1016/j.advwatres.2007.07.
- Gudmundsson L, Bremnes JB, Haugen JE, Skaugen TE. 2012. Technical note: downscaling RCM precipitation to the station scale using quantile mapping – a comparison of methods. *Hydrol. Earth Syst. Sci. Discuss.* **9**: 6185–6201, DOI: 10.5194/hessd-9-6185-2012.
- Hashmi MZ, Shamseldin AY, Melville BW. 2009. Statistical downscaling of precipitation: state-of-the-art and application of bayesian multi-model approach for uncertainty assessment. *Hydrol. Earth Syst. Sci.* **6**: 6535–6579, DOI: 10.5194/hessd-6-6535-2009.
- Hughes L. 2003. Climate change and Australia: trends, projections and impacts. *Aust. Ecol.* **28**: 423–443, DOI: 10.1046/j.1442-9993.2003.01300.x.
- Iizumi T, Nishimori M, Dairaku K, Adachi SA, Yokozawa M. 2011. Evaluation and intercomparison of downscaled daily precipitation indices over Japan in present-day climate: strengths and weaknesses of dynamical and bias correction-type statistical downscaling methods. *J. Geophys. Res. D: Atmos.* **116**: 1–21, DOI: 10.1029/2010JD014513.
- Ines AV, Hansen JW. 2006. Bias correction of daily GCM rainfall for crop simulation studies. *Agr. Forest. Meteorol.* **138**: 44–53, DOI: 10.1016/j.agrformet.2006.03.009.
- IPCC. 2000. *IPCC Special Report on Emissions Scenarios – Summary for Policymakers*. <http://www.ipcc.ch/pdf/special-reports/spm/sres-en.pdf>.
- Jeffrey SJ, Carter JO, Moodie KB, Beswick AR. 2001. Using spatial interpolation to construct a comprehensive archive of Australian climate data. *Environ. Model. Softw.* **16**: 309–330, DOI: 10.1016/S1364-8152(01)00008-1.

- Johnson F, Sharma A. 2009. Measurement of GCM skill in predicting variables relevant for hydroclimatological assessments. *J. Clim.* **22**: 4373–4382, DOI: 10.1175/2009JCLI2681.1.
- Johnson F, Sharma A. 2012. A nesting model for bias correction of variability at multiple time scales in general circulation model precipitation simulations. *Water Resour. Res.* **48**: 1–16, DOI: 10.1029/2011WR010464.
- Kalnay E, Kanamitsu M, Kistler R, Collins W, Deaven D, Gandin L, Iredell M, Saha S, White G, Woollen J, Zhu Y, Chelliah M, Ebisuzaki W, Higgins W, Janowiak J, Mo KC, Ropelewski C, Wang J, Leetmaa A, Reynolds R, Jenne R, Joseph D. 1996. The NCEP/NCAR reanalysis project. *Bull. Am. Meteorol. Soc.* **77**: 437–471, DOI: 10.1175/1520-0477(1996)077<0437:TNYRP>2.0.CO;2.
- Kharin VV, Zwiers FW. 2002. Climate predictions with multimodel ensembles. *J. Clim.* **15**: 793–799, DOI: 10.1175/1520-0442(2002)015<0793:CPWME>2.0.CO;2.
- Kunkel KE, Karl TR, Easterling DR, Redmond K, Young J, Yin X, Hennon P. 2013. Probable maximum precipitation and climate change. *Geophys. Res. Lett.* **40**: 1402–1408, DOI: 10.1002/grl.50334.
- Lafon T, Dadson S, Buys G, Prudhomme C. 2013. Bias correction of daily precipitation simulated by a regional climate model: a comparison of methods. *Int. J. Climatol.* **33**: 1367–1381, DOI: 10.1002/joc.3518.
- Li H, Sheffield J, Wood EF. 2010. Bias correction of monthly precipitation and temperature fields from Intergovernmental Panel on Climate Change AR4 models using equidistant quantile matching. *J. Geophys. Res. D: Atmos.* **115**: 1–20, DOI: 10.1029/2009JD012882.
- Maraun D, Wetterhall F, Ireson AM, Chandler RE, Kendon EJ, Widmann M, Brienen S, Rust HW, Sauter T, Themel M, Venema VKC, Chun KP, Goodess CM, Jones RG, Onof C, Vrac M, Thielen E. 2010. Precipitation downscaling under climate change: recent developments to bridge the gap between dynamical models and the end user. *Rev. Geophys.* **48**, DOI: 10.1029/2009RG000314.
- Meenu R, Rehana S, Mujumdar PP. 2013. Assessment of hydrologic impacts of climate change in Tunga-Bhadra river basin, India with HEC-HMS and SDSM. *Hydrol. Process.* **27**: 1572–1589, DOI: 10.1002/hyp.9220.
- Murphy J. 1998. An evaluation of statistical and dynamical techniques for downscaling local climate. *J. Clim.* **12**: 2256–2284, DOI: 10.1175/1520-0442(1999)012<2256:AEOSAD>2.0.CO;2.
- Nash JE, Sutcliffe JV. 1970. River flow forecasting through conceptual models, part 1 – a discussion of principles. *J. Hydrol.* **10**: 282–290, DOI: 10.1016/0022-1694(70)90255-6.
- Nasser M, Tavakol-Davani H, Zahraie B. 2013. Performance assessment of different data mining methods in statistical downscaling of daily precipitation. *J. Hydrol.* **492**: 1–14, DOI: 10.1016/j.jhydrol.2013.04.017.
- Ojha CSP, Goyal MK, Adeloye AJ. 2010. Downscaling of precipitation for lake catchment in arid region in India using linear multiple regression and neural networks. *Open Hydrol. J.* **4**: 122–136, DOI: 10.2174/1874378101004010122.
- Ojha R, Kumar DN, Sharma A, Mehrotra R. 2012. Assessing severe drought and wet events over India in a future climate using a nested bias correction approach. *J. Hydrol. Eng.* **18**: 760–772, DOI: 10.1061/(ASCE)HE.1943-5584.0000585.
- Panofsky HA, Brier GW. 1968. *Some Applications of Statistics to Meteorology*. PennState University: University Park, PA.
- Piani C, Haerter JO, Coppola E. 2010. Statistical bias correction for daily precipitation in regional climate models over Europe. *Theor. Appl. Climatol.* **99**: 187–192, DOI: 10.1007/s00704-009-0134-9.
- Prudhomme C, Crooks S, Kay AL, Reynard N. 2013. Climate change and river flooding: Part I classifying the sensitivity of British catchments. *Clim. Change.* **119**: 933–948, DOI: 10.1007/s10584-013-0748-x.
- Sachindra DA, Huang F, Barton AF, Perera BJC. 2013. Least square support vector and multi-linear regression for statistically downscaling general circulation model outputs to catchment streamflows. *Int. J. Climatol.* **33**: 1087–1106, DOI: 10.1002/joc.3493.
- Salvi K, Kannan S, Ghosh S. 2011. Statistical downscaling and bias-correction for projections of Indian rainfall and temperature in climate change studies. In *4th International Conference on Environmental and Computer Science*, 16–18 September 2011, Singapore, 7–11.
- Samadi S, Wilson CAME, Moradkhani H. 2013. Uncertainty analysis of statistical downscaling models using Hadley Centre Coupled Model. *Theor. Appl. Climatol.* **114**: 673–690, DOI: 10.1007/s00704-013-0844-x.
- Schnur R, Lettenmaier DP. 1998. A case study of statistical downscaling in Australia using weather classification by recursive partitioning. *J. Hydrol.* **213**: 362–379, DOI: 10.1016/S0022-1694(98)00217-0.
- Shao Q, Li M. 2013. An improved statistical analogue downscaling procedure for seasonal precipitation forecast. *Stochast. Environ. Res. Risk Assess.* **27**: 819–830, DOI: 10.1007/s00477-012-0610-0.
- Smith I, Chandler E. 2009. Refining rainfall projections for the Murray Darling basin of south-east Australia—the effect of sampling model results based on performance. *J. Clim. Change* **102**: 377–393, DOI: 10.1007/s10584-009-9757-1.
- Sun J, Chen H. 2012. A statistical downscaling scheme to improve global precipitation forecasting. *Meteorol. Atmos. Phys.* **117**: 87–102, DOI: 10.1007/s00703-012-0195-7.
- Teutschbein C, Seibert J. 2012. Bias correction of regional climate model simulations for hydrological climate-change impact studies: review and evaluation of different methods. *J. Hydrol.* **456–457**: 12–29, DOI: 10.1016/j.jhydrol.2012.05.052.
- Themebl MJ, Gobiet A, Leuprecht A. 2011. Empirical-statistical downscaling and error correction of daily precipitation from regional climate models. *Int. J. Climatol.* **31**: 1530–1544, DOI: 10.1002/joc.2168.
- Thomas P, Swaminathan A, Lucas RM. 2012. Climate change and health with an emphasis on interactions with ultraviolet radiation: a review. *Glob. Chang. Biol.* **18**: 2392–2405, DOI: 10.1111/j.1365-2486.2012.02706.x.
- Timbal B, Drosowsky W. 2013. The relationship between the decline of Southeastern Australian rainfall and the strengthening of the subtropical ridge. *Int. J. Climatol.* **33**: 1021–1034, DOI: 10.1002/joc.3492.
- Timbal B, Fernandez E, Li Z. 2009. Generalization of a statistical downscaling model to provide local climate change projections for Australia. *Environ. Model. Software* **24**: 341–358, DOI: 10.1016/j.envsoft.2008.07.007.
- Trenberth KE, Jones PD, Ambenje P, Bojariu R, Easterling D, Tank AK, Parker D, Rahimzadeh F, Renwick JA, Rusticucci M, Soden B, Zhai P. 2007. Observations: surface and atmospheric climate change. In *Climate Change 2007: The Physical Science Basis. Contribution of Working Group I to the Fourth Assessment Report of the Intergovernmental Panel on Climate Change*, Solomon S, Qin D, Manning M, Chen Z, Marquis M, Averyt KB, Tignor M, Miller HL (eds). Cambridge University Press: Cambridge, UK.
- Tripathi AK, Roberts CD, Eagle RA. 2009. Coupling of CO₂ and ice sheet stability over major climate transitions of the last 20 million years. *Science* **326**: 1394–1397, DOI: 10.1126/science.1178296.
- Victorian Government Department of Sustainability and Environment. 2008. *Climate change in the Wimmera*. Retrieved October 28, 2012. <http://www.climatechange.vic.gov.au/regional-projections/wimmera>.
- Wang W. 2006. *Stochasticity, Nonlinearity and Forecasting of Streamflow Processes*. Deft University Press: Amsterdam, the Netherlands.
- Wilby RL, Charles SP, Zorita E, Timbal B, Whetton P, Mearns LO. 2004. Guidelines for use of climate scenarios developed from statistical downscaling methods, supporting material to the IPCC. <http://www.ipcc-data.org/>.
- Wood AW, Leung LR, Sridhar V, Lettenmaier DP. 2004. Hydrologic implications of dynamical and statistical approaches to downscaling climate model outputs. *Clim. Change* **62**: 189–216, DOI: 10.1023/B:CLIM.0000013685.99609.9e.
- Yu PS, Yang TC, Wu CK. 2002. Impact of climate change on water resources in southern Taiwan. *J. Hydrol.* **260**: 161–175, DOI: 10.1016/S0022-1694(01)00614-X.
- Ziska LH, Bunce JA, Shimono H, Gealy DR, Baker JT, Newton PC, Reynolds MP, Jagadish KS, Zhu C, Howden M, Wilson LT. 2012. Food security and climate change: on the potential to adapt global crop production by active selection to rising atmospheric carbon dioxide. *Proc. R. Soc. Biol. Sci.* **279**: 4097–4105, DOI: 10.1098/rspb.2012.1005.